BBA - Molecular Cell Research 1871 (2024) 119786

Contents lists available at ScienceDirect

BBA - Molecular Cell Research

journal homepage: www.elsevier.com/locate/bbamcr

Review

Structural aspects of iron-sulfur protein biogenesis: An NMR view

Leonardo Querci [a,b], Mario Piccioli [a,b], Simone Ciofi-Baffoni [a,b,*], Lucia Banci [a,b,c,*]

[a] Magnetic Resonance Center CERM, University of Florence, Via Luigi Sacconi 6, Sesto Fiorentino, 50019 Florence, Italy
[b] Department of Chemistry, University of Florence, Via della Lastruccia 3, Sesto Fiorentino, 50019 Florence, Italy
[c] Consorzio Interuniversitario Risonanze Magnetiche di Metalloproteine (CIRMMP), Via Luigi Sacconi 6, Sesto Fiorentino, 50019 Florence, Italy

ARTICLE INFO

Keywords:
iron-sulfur cluster
NMR
Paramagnetism
ISC assembly machinery
CIA machinery
Mitochondria
Glutaredoxin
Ferredoxin

ABSTRACT

Over the last decade, structural aspects involving iron-sulfur (Fe/S) protein biogenesis have played an increasingly important role in understanding the high mechanistic complexity of mitochondrial and cytosolic machineries maturing Fe/S proteins. In this respect, solution NMR has had a significant impact because of its ability to monitor transient protein-protein interactions, which are abundant in the networks of pathways leading to Fe/S cluster biosynthesis and transfer, as well as thanks to the developments of paramagnetic NMR in both terms of new methodologies and accurate data interpretation. Here, we review the use of solution NMR in characterizing the structural aspects of human Fe/S proteins and their interactions in the framework of Fe/S protein biogenesis. We will first present a summary of the recent advances that have been achieved by paramagnetic NMR and then we will focus our attention on the role of solution NMR in the field of human Fe/S protein biogenesis.

1. Introduction

Since the early days of research on iron-sulfur (Fe/S) proteins, solution NMR spectroscopy has been successfully applied to Fe/S proteins for their characterization in terms of: i) electronic structure; ii) oxidation states and electron localization/delocalization over the cluster; iii) analysis of the magnetic coupling patterns among the iron ions of the Fe/S clusters; iv) their effects on the NMR spectra. It became thus clear that solution NMR spectroscopy applied to a highly paramagnetic system (paramagnetic NMR), in combination with EPR, Mössbauer and magnetic susceptibility measurements, is a precious tool for the characterization of the Fe/S cluster chemical-physical properties [1,2]. The pattern of the paramagnetic ^{1}H NMR spectra [3,4], the temperature dependence of the NMR signals [5], and their residue specific assignment [6–8] played an invaluable role for identifying the nature of the cluster, its overall oxidation state as well as that of each iron ion [6,9–11]. The integrated application of solution NMR with other spectroscopic techniques [12–15] constituted an exemplary case of their complementarity and opened one of the most popular playgrounds of modern structural biology applied to metalloproteins [16]. Paramagnetic NMR spectroscopy is informative on the electronic structure of the cluster as EPR spectroscopy does, it is highly sensitive to the oxidation and spin state, such as Mössbauer and electronic absorption spectroscopies do, and it provides all the above information at the same time on the same sample. Furthermore, the analysis of NMR chemical shift perturbations is a very efficient approach to study the interaction network of Fe/S proteins responsible of the Fe/S protein biogenesis [17–22]. The majority of the proteins involved into Fe/S cluster biogenesis are redox-sensitive, 10–40 kDa sized soluble proteins, thus being too small, and therefore not suitable, for cryo-electron microscopy (cryo-EM) investigations [23,24]. Of course, X-ray crystallography has been largely used to address structural aspects of Fe/S proteins and complexes involved in the Fe/S cluster biogenesis [25–32]. However, even when data are available with a very high resolution, there are some intrinsic limitations with X-ray structures: the redox state cannot be controlled, the presence of the bound cluster could be partial, and packing forces might affect the aggregation state thus making the crystal situation different from the active solution state of these proteins. On the other hand, the size of these Fe/S proteins is typically well suitable for NMR structural and interaction studies, and although the resolution of the NMR structures could be much lower than that of crystallographic data, solution NMR provides key information on the state of the protein that can easily complement the crystallographic picture of the system. There are no doubts that the NMR view on the structure and reactivity of Fe/S protein is unique, accurate and informative.

Paramagnetism is a common property of all Fe/S proteins in all

* Corresponding authors at: Magnetic Resonance Center CERM, University of Florence, Via Luigi Sacconi 6, Sesto Fiorentino, 50019 Florence, Italy.
E-mail addresses: ciofi@cerm.unifi.it (S. Ciofi-Baffoni), banci@cerm.unifi.it (L. Banci).

https://doi.org/10.1016/j.bbamcr.2024.119786
Received 13 February 2024; Received in revised form 15 May 2024; Accepted 10 June 2024
Available online 18 June 2024

oxidation states, because in no case a Fe/S cluster can be treated as diamagnetic at room temperature. Some cluster types and oxidation states are characterized by an S = 0 ground state of the electron spin energy ladder, but excited states are thermally accessible. The consequence is that, at room temperature, also systems with a S = 0 ground state, and therefore EPR silent at low temperature, such as $[2Fe\text{-}2S]^{2+}$ or $[4Fe\text{-}4S]^{2+}$ clusters, do exhibit a remarkable paramagnetism that can be quantified and accounted for on the basis of the paramagnetic NMR spectral properties. The interaction between the electron and the nuclear spins is described by a term of the spin Hamiltonian called hyperfine coupling [33]. The hyperfine coupling gives rise to contributions to the chemical shifts and to the relaxation rates of nuclear spins, which sum up to those of the same system in the diamagnetic state. The paramagnetic effects on the spectral parameters can be detected and quantified using tailored NMR approaches [34]. The presence of a paramagnetic center brings pro's and con's into the NMR characterization, both of them widely discussed in the current literature [35–42]. The additional contributions to nuclear spin relaxation arising from the electron spin-nuclear spin interaction may broad NMR lines beyond detection, thus bleaching out NMR signals of nuclear spins that are (too) close to the metal center. On the other hand, the information arising from the hyperfine coupling acts as a very accurate fingerprint of the type of cluster, coordination sphere, oxidation states of the individual iron ions, valence localization/delocalization, magnetic coupling [43–46].

We are going here to describe the use of solution NMR in characterizing the structural aspects of Fe/S proteins and their interactions in the framework of Fe/S protein biogenesis. We will first present a summary of the recent advances that have been achieved by paramagnetic NMR and then we will focus our attention on the impact of solution NMR in the field of Fe/S protein biogenesis. This review aims at showing how solution NMR spectroscopy has contributed to the in vitro identification of many snapshots of the [2Fe-2S] and [4Fe-4S] assembly and transfer processes and how it could still help in the future to unravel the molecular mechanism of iron-sulfur protein biogenesis, which are still far from being fully understood.

2. Dedicated paramagnetic NMR methodologies

The theory of the hyperfine coupling between electron spins and nuclear spins has been exhaustively reviewed, also reporting the relevant equations, which do not need to be reiterated here [36,47,48]. The hyperfine shift, i.e. the contribution to the chemical shift arising from the hyperfine coupling, is determined by a pseudo-contact shift (PCS) and by a contact shift (CS) contribution. The former arises from the motional average of the dipole-dipole interaction between the nuclear and the electron magnetic moments. In solution, this contribution is different from zero only in presence of an anisotropic paramagnetic susceptibility tensor. Due to its dipolar nature, the PCS contribution also depends on r^{-3} with r being the metal-to-nucleus distance. The magnetic susceptibility anisotropy of Fe^{3+}/Fe^{2+} high spin ions in tetrahedral geometry [33,49] is small enough to neglect, at least in a first approximation, PCS contributions to the chemical shift. Under the assumption that the magnetic anisotropy of each individual Fe ion of the cluster is not affected by the magnetic coupling, one can safely assume that the paramagnetic shift in Fe/S proteins, for the various cluster types, is essentially due to the contact contribution(s). The CS contribution depends on the unpaired electron spin density localized on the resonating nucleus. The latter has sizable values only for the nuclei of the ligands directly coordinated to the paramagnetic metal ion(s) or of groups interacting with them through H-bonds.

2.1. Exploiting magnetically coupled iron ions in Fe/S proteins for structural characterization

In Fe/S proteins, the Fe^{3+}/Fe^{2+} ions are magnetically coupled and give rise to peculiar effects on the NMR data. The magnetic coupling between two or more paramagnetic ions gives rise to new electron spin levels, whose energy depends on the oxidation and spin state of the metal ions and on the values of the magnetic coupling constant J [5]. The observed contact shift arises from the sum of the hyperfine coupling for each spin level, weighted for the population of the spin levels, according to the Boltzmann distribution (Fig. 1A) [47]. Consequently, CS are a very sensitive probe of the type of cluster, of its oxidation state and of the valence distribution within the cluster, as summarized in Fig. 1B. Once the nature of the cluster is identified from the general pattern of paramagnetic signals, the residue-specific assignment of signals from cluster-bound residues can be used to obtain information on the dihedral angle of residues coordinating the metal center [8] and on the number of H-bonds surrounding the cluster [50].

A paramagnetic center can also significantly affect the nuclear spin relaxation properties. The paramagnetic contribution to nuclear spin relaxation rates is determined by various terms: contact, dipolar and Curie spin relaxation. For nuclei outside the first coordination sphere, therefore not experiencing electron spin density on them, the contact contribution is null and nuclear spin relaxation is only determined by through-space interactions, as both dipolar and Curie spin relaxation terms are. They have an r^{-6} dependence, being r the distance between the metal ion and the nuclear spins.

The magnetic coupling among metal ions, determining new spin states, affects the nuclear spins as well as the electron spin relaxation properties [51]. For a multiple coupled metal ions system, each nuclear spin is affected by all metal ions of the system; however, the equations describing the contact, the dipolar and the Curie spin relaxation contributions are modified by taking into account the new electron spin levels of the coupled system [47]. New transitions involving electron spin levels can occur, therefore the electronic relaxation times of the metal ions change under the effect of the magnetic coupling(s). Depending on the spins involved in the coupling (if they are equal, Fe(III)-Fe(III) or different, Fe(III)-Fe(II)) and on the extent of the magnetic coupling, as different behaviours are expected for $J/kT >> 1$ or $J/kT << 1$), very different patterns may arise and, indeed, relaxation properties in magnetically coupled systems constitute, essentially, a fingerprint of each different cluster and oxidation state (Fig. 1) [5,11].

Several approaches have been proposed to convert R_1 and R_2 nuclear relaxation rates into structural restraints; the most used approach is based on the assumption that, neglecting contact contribution, paramagnetic relaxation can be treated as $R_{1,2} = \sum_i \frac{K_{1,2}}{r_i^6}$, where r_i is the distance between the nuclear spin and the Fe_i of the cluster. The constants $K_{1,2}$ contain all the terms that appear in the Solomon equation, which are difficult to predict in a magnetically coupled system. However, when a sufficient number of R_1 or R_2 relaxation rates are available, values of $K_{1,2}$ can be obtained from the fitting and the equation used to convert relaxation rates into structural restrains [52]. This relationship has been, and still is being, exploited for the conversion of paramagnetic relaxation enhancements into metal-to-nucleus distance restraints for structure calculations [52–57].

NMR-based approaches dedicated to the solution structures of paramagnetic proteins have been developed in the 90'es and, since them, widely used to obtain the NMR structure of different Fe/S proteins [58]. The general approach is to combine standard NMR restraints (nuclear Overhauser effect, dihedral angles, chemical shift index), with paramagnetism based NMR restraints (dihedral angles, 1D nuclear Overhauser effect from paramagnetic signals, paramagnetic relaxation enhancement effects, H-bonds involving unpaired spin density from the cluster). When successful, the combination of classical and paramagnetism-based NMR restraints provides small root-mean-square deviation values throughout the structure, including the regions that are very close to the paramagnetic center. However, depending on the size of the protein and on the type of cluster, there might be cases in which the signal broadening due to the paramagnetic center causes a

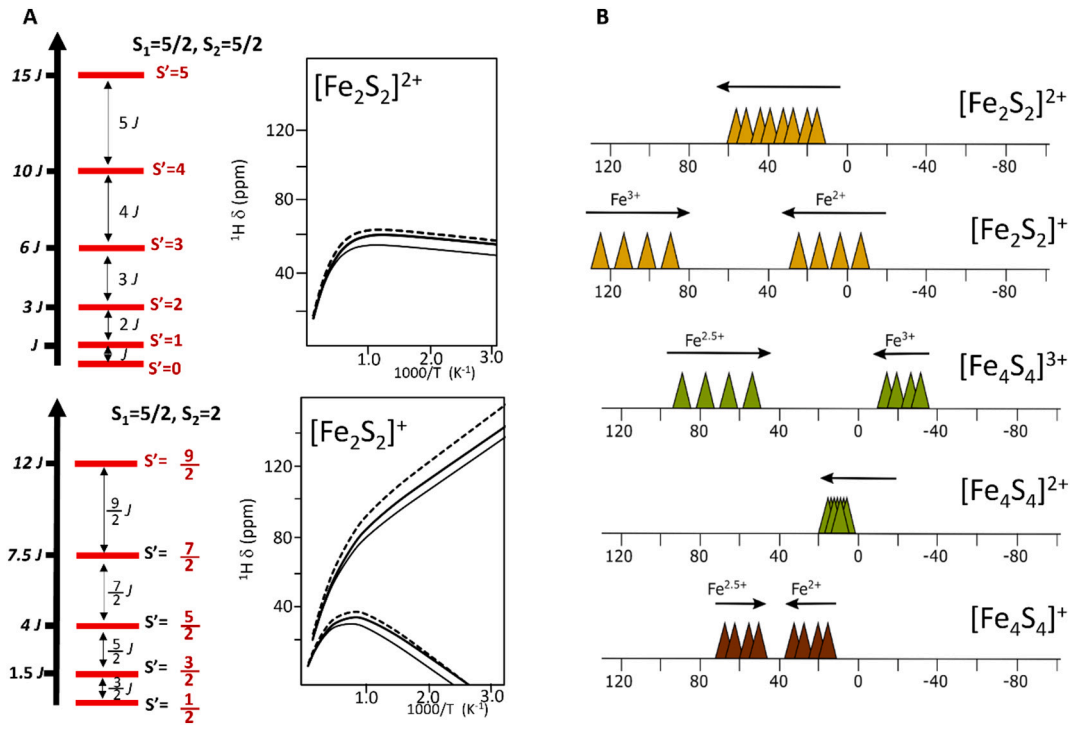

Fig. 1. Antiferromagnetic coupling and NMR properties. A) Left: Energy level diagrams for oxidized (top) and reduced (bottom) [2Fe-2S] clusters. $S_{1,2}$ are the electron spin of the uncoupled iron ions, S′ refers to the electron spin of the coupled system. Right: Calculated temperature dependence of the paramagnetic shifts of βCH_2 signals of the ligands, obtained considering $J = 200\ cm^{-1}$ and A = 1.81 MHz. The thin and dashed lines report an increase of 10 % of the exchange coupling constant or of the hyperfine electron-nuclear coupling, respectively. B) Schematic drawing of expected chemical shift values for βCH_2 signals of the ligands in [2Fe-2S] and [4Fe-4S] clusters. Arrows indicate the direction of change in chemical shift of the signals upon temperature increase [38].

"blind sphere" around the cluster that severely limits the quality of the structure in the proximity of the prosthetic group.

More recently, solution NMR has demonstrated its ability in characterizing at the atomic level protein-protein interaction networks involved in Fe/S cluster assembly and transfer. In particular, solution NMR spectroscopy has been successfully applied to weak or transient protein-protein interactions [59], which are abundant in the networks of protein-protein interactions leading to Fe/S cluster biosynthesis and transfer [11,20,60], and they will be extensively described in Section 3.

2.2. Application of ^{13}C-direct detection to characterize challenging Fe/S proteins

In the last two decades, the NMR approach for the structure of metalloproteins has been implemented with the development of ^{13}C detected experiments [56,61–66]. Their rationale is based on the fact that paramagnetic relaxation depends on the square of the gyromagnetic ratio of the studied nucleus [47,67], therefore paramagnetic relaxation effects are 16 times lower for ^{13}C spins than for ^{1}H spins. Therefore, residues whose ^{1}H signals are broadened beyond detection may have the corresponding ^{13}C signals still detectable. This has been successfully applied, among the several systems, to the NMR characterization of MitoNEET (or CISD1) [68]. Particularly, tailored CACO and CON experiments have been tested on both oxidized and reduced states of CISD1, giving rise to a significant decrease of the blind sphere around the cluster (Fig. 2A and B) [68,69]. It has been shown that the interplay between structure and NMR assignment can be exploited in the "reverse" approach to extend the NMR resonance assignment. In paramagnetic proteins, the sequential assignment strategy is not applicable in the surrounding of the metal centers, because paramagnetic relaxation makes the scalar connectivities, needed for an unambiguous signal assignment, non-detectable. However, it is often possible, via tailored experiments, to observe signals arising from the proximity of the metal center (Fig. 2C and D) [70,71]. Typically, scalar and dipolar connectivities involving these signals are not detected; however, nuclear spin relaxation rates can be measured and used to obtain metal-to-nucleus distances. When a reliable structural model of the protein is available, the distance from the metal center can be used to assign the signal, without any sequential connectivity.

As outlined above, paramagnetic relaxation is less efficient on carbon spins than on the proton spins; therefore, the range of distances monitored by ^{13}C paramagnetic relaxation rates can be effectively combined with that of ^{1}H paramagnetic relaxation rates and, together, strongly reinforces the battery of paramagnetism based structural restraints. The R_1 and R_2 rates of $^{13}C\alpha$ and $^{13}C'$ can be measured via a battery of recently developed experiments [34,71] and, together with an extensive combination of classical and paramagnetic based structural restraints, they succeeded to obtain NMR structures [57,72] sufficiently in all protein regions.

3. Solution NMR contributions to the mechanism of Fe/S cluster assembly and transfer in human mitochondrial ISC assembly and CIA machineries

In the following sections, we present recent advances and contributions that solution NMR has made toward the molecular understanding of Fe/S protein biogenesis in the human mitochondrial iron-sulfur cluster (ISC) assembly machinery and in the human cytosolic iron-sulfur protein assembly (CIA) machinery.

3.1. Mitochondrial ISC assembly machinery: [2Fe-2S] cluster assembly on a scaffold protein

A large complex (termed here the core ISC complex) assembles [2Fe-2S] clusters in the mitochondrial matrix. This complex is formed by six proteins (ISCU2, ACP1, ISD11, NFS1, FXN, FDX2) and, within this

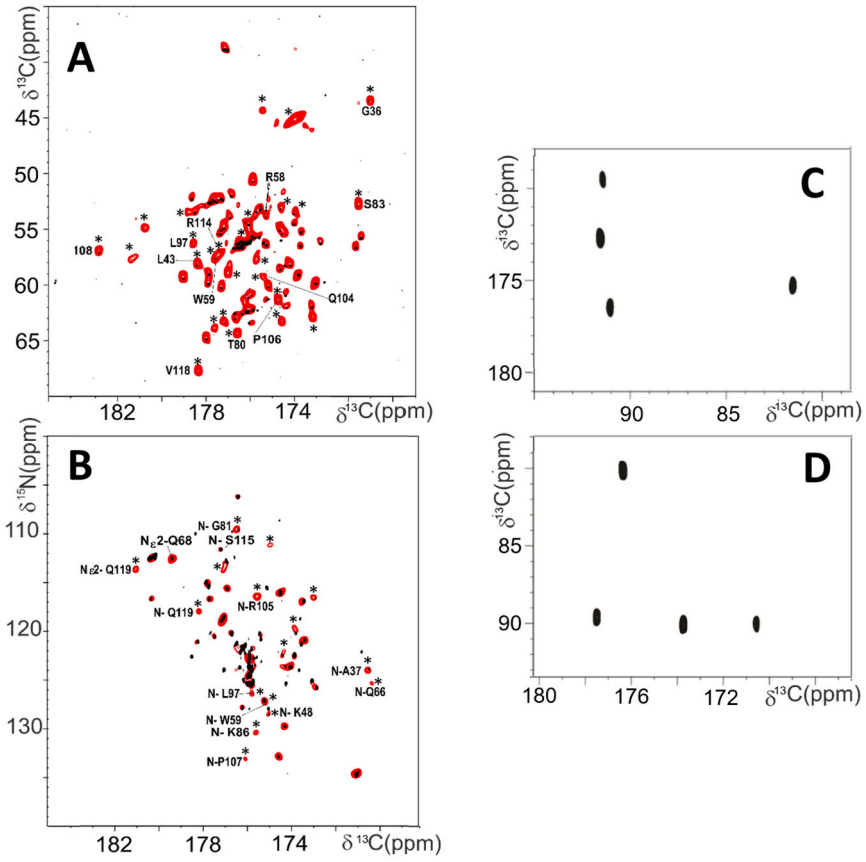

Fig. 2. Optimization of ^{13}C-direct detection experiment for paramagnetic systems. Overlay of diamagnetic CACO (black) and paramagnetic CACO (red) (A) and overlay of diamagnetic CON (black) and paramagnetic CON (red) (B). Experiments have been performed, at 175 MHz Larmor Frequency using a Bruker Avance NEO 700 spectrometer, on the protein CISD3, containing two [2Fe-2S] clusters in the reduced, $[Fe_2S_2]^+$ state. Asterisks represent the extra paramagnetic signals that are not seen in the diamagnetic experiments. The chemical shift assignments obtained thanks to the paramagnetic experiments are indicated [70]. COCA-AP (C) and CACO-AP (D) spectra, recorded to identify the C^{α}/C' signals of iron bound cysteines. Experiments have been performed, at 300 MHz Larmor Frequency using a Bruker Ascend NEO 1200 spectrometer, on the HiPIP protein PioC, containing a [4Fe-4S] cluster in the $[Fe_4S_4]^{2+}$ state. The relative intensity of the peaks in the two experiments provide information about the orientation of the C^{α}-C′ backbone bond with respect to the iron ion [71].

complex, ISCU2 acts as a scaffold protein providing the molecular unit collecting and assembling ferrous ions and sulfur atoms into a [2Fe-2S]$^{2+}$ cluster (Fig. 3A). The structural arrangement of the core ISC complex has been visualized few years ago by several studies applying several techniques including NMR [73–75]. On this respect, the ^{1}H-^{15}N TROSY HSQC-based NMR studies contributed to provide structural restraints to determine how frataxin (FXN) interacts within the core ISC complex [74,76]. When FXN is titrated with stoichiometric amounts of dimeric NFS1:ISD11:Acp complex, H^N-N^H cross-peaks, shift, broaden and disappear. These effects on the NMR spectrum are envisaged when FXN binds the large molecular complex formed by dimeric NFS1:ISD11:Acp and adopts the tumbling time of the NFS1:ISD11:Acp:FXN complex. Upon addition of ISCU2 to the obtained NFS1:ISD11:Acp:FXN complex, FXN signal shifting, broadening, and disappearing increases. The chemical shift perturbation analysis of the NMR spectra revealed that FXN residues interacting with the dimeric NFS1:ISD11:Acp complex are placed on helix α1 and strand β1 and that, after the addition of ISCU2, major chemical shift perturbations appeared in the β-sheet region of FXN [74]. Overall, NMR spectroscopy is unique in indicating that, in vitro, ISCU2 and FXN proteins cooperate in the interaction to the complex, and that FXN binds more strongly to the dimeric NFS1:ISD11:Acp complex in the presence of ISCU2. Furthermore, solution NMR studies contribute to investigate the molecular function of FXN in the mitochondrial ISC assembly machinery. This protein was first suggested to be a metallochaperone providing Fe^{2+} ions required to assemble the [2Fe-2S] cluster on the core ISC complex [77–80]. The NMR studies supporting this model indicated that FXN binds Fe^{2+} at a negatively charged helix [78] but not Fe^{3+}, and that Fe^{2+}-FXN binds to the dimeric NFS1:ISD11:Acp complex with no iron release. Moreover, once the sulfide is formed by the complex either adding reduced FDX2 or dithiothreitol (DTT), Fe^{2+} is released from FXN because of its oxidation to Fe^{3+} [76]. On the other hand, the cryo-EM structure of the human NFS1:ISD11:ACP1:ISCU2:FXN complex [75] (Fig. 3A) showed that iron-binding site of FXN is far from where the [2Fe-2S] cluster synthesis occurs, thus contradicting the functional role of FXN as metallochaperone in the mechanism. Several studies from different labs deny, indeed, the model of FXN as iron chaperone and propose that FXN is only an allosteric activator of the persulfide transfer process [81,82]. The finding that an ISCU2 genetic mutant (M108I) can survive with no need of frataxin also support that FXN does not work as iron donor [83–85]. On this respect, NMR played a fundamental role to explain the mechanism of the ISCU2 mutant that bypasses FXN [86]. The ^{1}H-^{15}N HSQC spectrum showed that ISCU2(M108) variant is almost completely structured, while wild-type ISCU2 exists in two interconverting conformations, i.e. a structured form (S-state) and a dynamically disordered form (D-state) [86,87]. Upon titration of ISCU2 with unlabelled dimeric NFS1:ISD11:Acp complex, M108 mutant of ISCU2 is able to interact with high affinity to generate a [2Fe-2S] cluster. In this case, FXN does not act as an allosteric modulator that increase the rate of the assembly reaction, as instead it occurs for the wild-type ISCU2 [86]. This is because, after dimeric NFS1:ISD11:Acp:ISCU2:FXN complex formation, the binding of reduced ferredoxin FDX2, displaces FXN. This mechanism became evident when

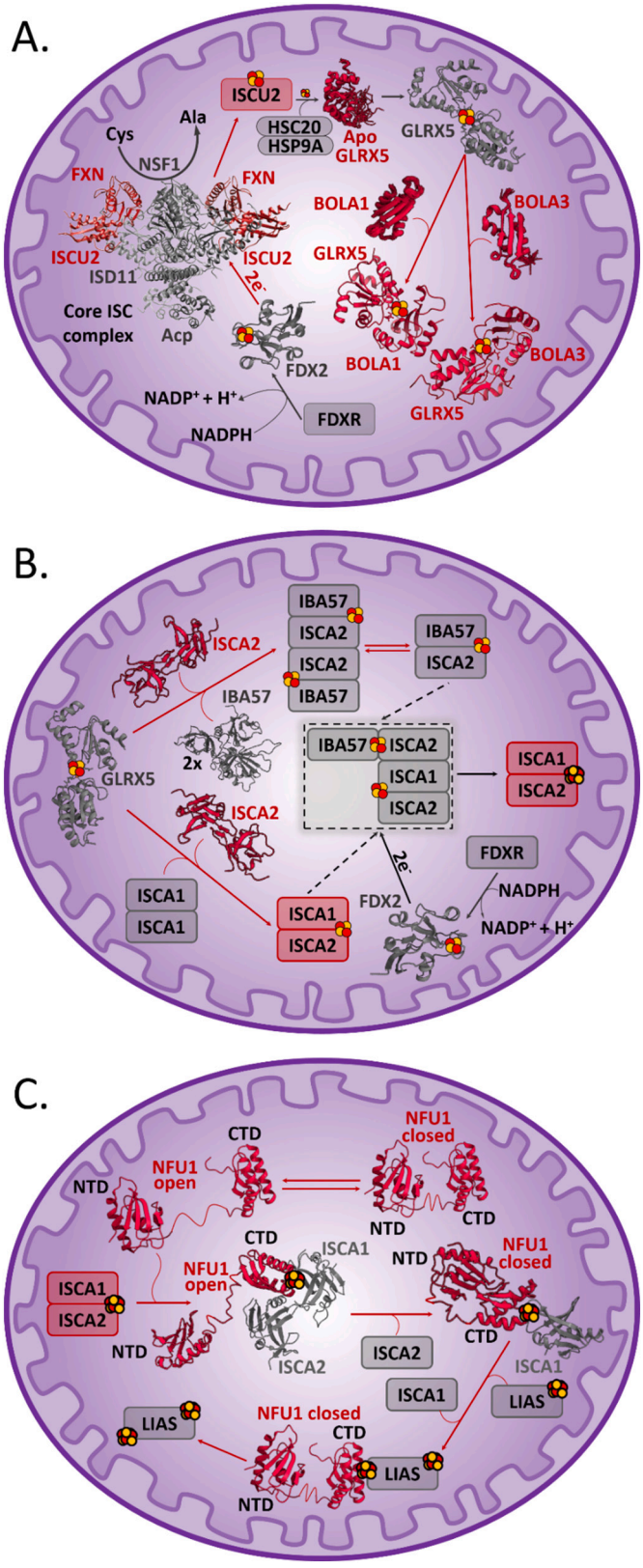

(caption on next column)

Fig. 3. Molecular model of mitochondrial Fe/S protein biogenesis based on integrated structural biology data. A) Assembly of [2Fe-2S] cluster on ISCU2 driven by the core ISC complex and [2Fe-2S] cluster trafficking to GLRX5 and GLRX5-BOLAs complexes. PDB IDs are: ISC complex-5WLW, apo-GLRX5-2MMZ, [2Fe-2S] GLRX5-2WUL, BOLA3-2NCL, BOLA1-5LCI, [2Fe-2S] FDX2-2Y5C. B) Generation of [4Fe-4S] cluster on ISCA1-ISCA2 complex. Dashed rectangle and arrows indicate a putative working model for [2Fe-2S] reductive coupling mechanism. PDB ID for IBA57 is 6QE3. C) Transfer of [4Fe-4S] cluster to LIAS. PDB IDs are: NFU1-CTD-2M5O and NFU1-NTD-2LTM. Red colors were used to highlight proteins and pathways that have been characterized through solution NMR. Structural models of human proteins, solved by X-ray crystallography, solution NMR or information-driven flexible docking approaches were reported. [2Fe-2S] and [4Fe-4S] clusters were represented as red (for Fe) and yellow (for S) spheres.

^{1}H-^{15}N TROSY HSQC NMR spectra of FXN were recorded following the two-step addition of: i. dimeric NFS1:ISD11:Acp:ISCU2 complex, ii. FDX2. Sharp H^{N}-N^{H} cross peaks of isolated FXN, shift and/or broaden beyond detection when dimeric NFS1:ISD11:Acp:ISCU2 complex is added, but the totality of the signals is recovered after the addition of FDX2, indicating the complete dissociation of FXN from the core ISC complex [86]. This scenario agrees with recent data indicating that yeast homologues of FDX2 and FXN (i.e. Yah1 and Yfh1) bind to the yeast cysteine desulfurase Nfs1 using the same binding site and display a mutually exclusive binding [88]. The same was also observed for bacterial ferredoxin and frataxin, which mutually exclusively bind to the bacterial IscS-IscU complex [89].

A further contribution of solution NMR to dissect the mechanism of [2Fe-2S] cluster assembly on the core ISC complex concerns the formation of the sulfide ions (S^{2-}) driven by the cysteine desulfurase NFS1 and the electron donor FDX2. Two electrons are required to reduce persulfide sulfurs, formed by NFS1, to sulfides (Fig. 3A). It has been demonstrated that the electron donor is FDX2, whose [2Fe-2S] cluster is reduced by the ferredoxin reductase FDXR, which receives electrons from NADPH (Fig. 3A) [90,91]. FDX2, within the core ISC complex, is in charge of donating at least one of the two required electrons [90–92]. Oxidized and reduced FDX2 have distinct ^{1}H-^{15}N HSQC NMR spectra, where most of the differences involve residues close to the [2Fe-2S] cluster-binding site [93]. The ^{1}H-^{15}N HSQC NMR spectra differ between oxidized and reduced states, which can be thus used to monitor electron transfer processes at atomic resolution. The electron transfer process can be also monitored by paramagnetic 1D ^{1}H NMR. Thanks to paramagnetic tailored NMR experiments, the hyperfine-shifted resonances of oxidized and of reduced FDX2 have been acquired [93]; their shifts and temperature dependence directly reflects the oxidation state of the cluster [11]. Furthermore, since the electron exchange between the reduced and the oxidized form is slow on the NMR time-scale [94], both ^{1}H-^{15}N HSQC NMR and paramagnetic 1D ^{1}H NMR spectra provide information about the exchange rate of the electron transfer process. By applying these NMR experiments, the reduced form of the yeast homologue of FDX2 (Yah1) shows significantly higher affinity for the yeast homologue of ISCU2 (Isu1) than the oxidized form. NMR data also identified the interaction surface between Isu1 and Yah1, indicating a possible pathway of the electrons from reduced Yah1 to Isu1 [95]. NMR studies have also been used to demonstrate that both reduced and oxidized FDX2 recognize dimeric NFS1:ISD11:Acp complex [93], that electrons were provided by reduced FDX2 to generate sulfur, and that a highly conserved region close to the [2Fe-2S] clusters of FDX2 forms the interaction site in the complex. As helix α3 has been shown to bind to both the complex and FDXR [96], it results that FDX2 bound to the dimeric NFS1:ISD11:Acp complex cannot be reduced by FDXR, but it needs to disrupt its interaction with the complex in order to interact with another FDXR molecule and to receive the second electron required to complete the assembly of the [2Fe-2S] cluster on ISCU2. NMR data finally showed that FDX1 binds to the complex less tightly than FDX2 and yields Fe/S cluster assembly less rapidly [93]. Thus, FDX2 was demonstrated to be the physiological electron donor in mitochondrial ISC assembly machinery from both in vitro [90] and in vivo [91] works.

3.2. Mitochondrial ISC assembly machinery: [2Fe-2S] cluster transfer from ISCU2 to target apo proteins via GLRX5

Once the [2Fe-2S] cluster is assembled, the monothiol glutaredoxin-5 (GLRX5) receives the [2Fe-2S] cluster from ISCU2. GLRX5 is a component of the mitochondrial ISC assembly machinery [97], which distributes the [2Fe-2S] cluster to target apo proteins. These are both mitochondrial proteins requiring [2Fe-2S] clusters for their function and accessory proteins involved in the assembly of [4Fe-4S] clusters. This transfer reaction depends by dedicated molecular chaperones [98,99], which, in humans, are the mitochondrial ATP-dependent HSPA9 and HSC20 proteins (Fig. 3A) [100,101]. The mechanism of the transfer of the [2Fe-2S] cluster from ISCU2 to GLRX5 mediated by this chaperone/co-chaperone system is unknown. NMR studies provided some hints on how the HSPA9-HSC20 chaperone-cochaperone system interacts with ISCU2 [102], but still this process is not well characterized at the atomic level. Many recent research studies have been, however, performed to investigate the chaperone-cochaperone function in Fe/S protein biogenesis [103], but they will not be discussed here, as they did not apply NMR spectroscopy.

In the last decade, solution NMR were applied to address how [2Fe-2S] GLRX5 operates in the transfer of its cluster to protein partners. GLRX5 belongs to the monothiol glutaredoxin family, which has a conserved a CysGlyPheSer active site, which typically coordinates a [2Fe-2S] cluster bridged in a homodimeric complex [104]. Monothiol glutaredoxins can also form [2Fe-2S]-bridged complexes involving BolA proteins. BolA protein family typically has an invariant C-terminal His and an extra His or Cys residue which act as cluster ligands [105]. The NMR solution structure of the apo form of GLRX5 has been solved by us [106] showing that i) the protein is monomeric in solution, ii) the conserved Cys is highly solvent exposed, and iii) GSH interacts with GLRX5 in a specific binding site close to the conserved Cys. We showed that [2Fe-2S] cluster binding promotes GLRX5 dimerization. This is because the $[2Fe\text{-}2S]^{2+}$ cluster bridges two subunits of GLRX5 thanks to the coordination of a conserved Cys and a GLRX5-bound GSH molecule per GLRX5 unit, resulting a high solvent accessible cluster (Fig. 3A). Furthermore, paramagnetic NMR experiments (^{1}H-^{15}N IR-HSQC-AP and 1D ^{13}C NMR) showed two sets of peaks for some residues of the Fe/S cluster binding site, indicating that dimeric [2Fe-2S] GLRX5 adopts in solution two conformations [106,107]. This NMR description indicated that GLRX5 has molecular features suitable to transfer a [2Fe-2S] cluster to apo target proteins. A stable binding of the [2Fe-2S] cluster is, indeed, associated with its kinetic lability determined by a solvent-accessible metal binding site, which can promote a ligand exchange mechanism.

Two mitochondrial BOLA proteins (BOLA1 and BOLA3) are present in humans [108]. Patients with BOLA3 mutations show biochemical phenotypes similar to those of patients with mutations present in NFU1, another protein of the mitochondrial ISC assembly machinery [109,110]. This data has suggested that BOLA3 plays a role with NFU1 in the machinery. In addition, BOLA1 was suggested to be involved in the mitochondrial ISC assembly machinery as it is co-purified with GLRX5 [111]. Although, based on yeast studies [19], it might be expected that BOLA1 and BOLA3 facilitate the transfer and insertion of [4Fe-4S] clusters into target apo proteins, their role in the mitochondrial ISC assembly machinery and their position in the pathway are still elusive. BOLA1 and BOLA3 proteins are monomeric in solution and interact with apo GLRX5 forming an apo dimeric complex [19]. NMR studies indicate that BOLA3 and BOLA1 have very similar affinities with apo GLRX5, and that the residues nearby the conserved His in BOLAs and the GSH binding site in GLRX5 form the interaction site in both apo GLRX5-BOLA1 and apo GLRX5-BOLA3 complexes [19]. By NMR, it was also observed that homodimeric [2Fe-2S] GLRX5 interact with both BOLA1 and BOLA3 promoting the formation of monomeric apo GLRX5 and of a GLRX5-BOLAs complex bridging a [2Fe-2S] cluster (Fig. 3A). Chemical shift changes very similar to those observed in apo complexes were observed in the formation of the [2Fe-2S] GLRX5-BOLAs complexes, but with additional chemical shift changes detected for His67 of BOLA1, Cys59 of BOLA3 and the conserved Cys67 of GLRX5. These regions were the same identified in the formation of the [2Fe-2S] GLRX5 homodimer, showing that homo and heterodimers interact similarly. Spectroscopic data indicated that, for both BOLA1-GLRX5 and BOLA3-GLRX5 complexes, the [2Fe-2S] cluster is coordinated by a GLRX5-bound GSH molecule, the conserved Cys of GLRX5, by the invariant His of BOLA1 or BOLA3 and by a Cys or a His in BOLA3 and BOLA1, respectively [112]. NMR data also showed that both [2Fe-2S] BOLA1-GLRX5 and [2Fe-2S] BOLA3-GLRX5 complexes are more stable than the [2Fe-2S] GLRX5 homodimeric complex, and that, at variance of what occurs for the formation of the apo complexes, the [2Fe-2S] GLRX5-BOLA1 complex is preferentially formed with respect to [2Fe-2S] GLRX5-BOLA3, thus being the different BOLA1 vs. BOLA3 ligands the discriminating factor [112]. Structural models of the two complexes showed that the [2Fe-2S] BOLA3-GLRX5 complex exposes the cluster to solvent more than what it occurs in the [2Fe-2S] BOLA1-GLRX5 complex (Fig. 3A) [112]. This information indicates that the [2Fe-2S] BOLA3-GLRX5 complex works as a metallochaperone promoting to cluster-exchange with GLRX5-partner proteins, similarly to what observed for homodimeric [2Fe-2S] GLRX5. This scenario is in agreement with recent data showing that the two mitoribosome subunits receive [2Fe-2S] clusters via a GLRX5-BOLA3 pathway [113] as well as to other apo acceptors [114,115]. On the contrary, the [2Fe-2S] cluster in the BOLA1-GLRX5 complex is less solvent accessible and actively works as redox center. This information supports that the [2Fe-2S] BOLA1-GLRX5 complex functions as electron transfer carrier and not as a metallochaperone. The no [2Fe-2S] cluster trafficking role of the [2Fe-2S] BOLA1-GLRX5 complex is supported by in vitro studies showing that the complex does not transfer the cluster to apo protein acceptors [116].

3.3. Mitochondrial ISC assembly machinery: [4Fe-4S] cluster assembly

Several studies showed that the human proteins ISCA1, ISCA2, IBA57 are involved in the assembly of a [4Fe-4S] cluster in mitochondria [117–120], and others showed that human GLRX5 is a protein partner of human ISCA proteins [121,122]. NMR studies from our laboratory provided the first clear evidence that GLRX5 is the metallochaperone donating its bound [2Fe-2S] cluster to ISCAs [17,106,123]. GLRX5 interacts, indeed, with both ISCA1 and ISCA2, and one of the two conformers of [2Fe-2S] GLRX5 preferentially donates the [2Fe-2S] cluster to ISCA1 and ISCA2. NMR studies also showed that a dimeric complex is formed by apo ISCA1 and apo ISCA2, which, upon receiving two $[2Fe\text{-}2S]^{2+}$ clusters from two [2Fe-2S] GLRX5 molecules, can form a $[4Fe\text{-}4S]^{2+}$ cluster by reductive coupling when high concentrations of DTT and GSH are present. This process is not operative on the ISCA homodimeric complexes. These NMR-based findings thus demonstrated that the ISCA1-ISCA2 dimeric complex is the module assembling [4Fe-4S] clusters in mitochondria (Fig. 3B) [17]. A NMR study also allowed us to propose a molecular model of the mechanism of [4Fe-4S] cluster formation on the ISCA1-ISCA2 heterodimeric complex [123]. In this study, it was shown that the two C-terminal cysteines present in the C-terminus of homodimeric ISCA2 can sequentially extract two $[2Fe\text{-}2S]^{2+}$ clusters from GLRX5. It was suggested that the high structural flexibility of the C-terminal tails of ISCA1 and ISCA2 [17] drives the formation of an intermediate formed by a cluster-bridged GLRX5-ISCA1-ISCA2 complex with two bound $[2Fe\text{-}2S]^{2+}$ clusters. This intermediate might be the crucial species able to promote the reductive coupling of the two [2Fe-2S] clusters bound to it [106], upon accepting two electrons from DTT, to form the $[4Fe\text{-}4S]^{2+}$ cluster bound to the ISCA1-ISCA2 complex. This mechanism, however, did not explain the essential role of IBA57 in the [4Fe-4S] cluster assembly process. Recently, a DTT-free in vitro reconstitution system [124], which used GLRX5 as a [2Fe-2S] donor and mitochondrial aconitase as a [4Fe-4S] acceptor, showed that IBA57 is absolutely required to form the $[4Fe\text{-}4S]^{2+}$ cluster, although it does not clarify its molecular role. Moreover, this study defines that the electron

transfer pathway providing the two electrons required to form the [4Fe-4S]$^{2+}$ cluster on ISCA1-ISCA2 complex is formed by FDX2, its reductase FDXR, and NADPH (Fig. 3B). FDX1, the other ferredoxin present in the mitochondrial matrix cannot replace FDX2 in this process, in agreement with in vivo studies performed on the two ferredoxins [91,92,125,126], which indicated a distinct role of the two human ferredoxins. We recently showed by NMR and analytical gel filtration that a stable heterodimeric complex is formed by IBA57 and ISCA2 (but not by ISCA1), only once a [2Fe-2S] cluster bridges the two proteins [127]. The ligands of the [2Fe-2S] cluster are a conserved cysteine of IBA57 (Cys 230), which characterizes IBA57 protein family, and three conserved cysteines, which characterize the ISCA protein family. When IBA57 is mixed either to [2Fe-2S] ISCA2 or to [2Fe-2S] GLRX5 and apo ISCA2, the same [2Fe-2S] IBA57-ISCA2 complex is formed. Thus, this study delineates a GLRX5\ISCA2\IBA57-dependent pathway that brings to the assembly of a [2Fe-2S] ISCA2-IBA57 complex (Fig. 3B). We also found that the [2Fe-2S] cluster bound to this heterocomplex can switch from its reduced to oxidized states. This finding suggests that the binding of IBA57 to the [2Fe-2S] cluster activates a reduction process on the [2Fe-2S] cluster bound to ISCAs. Thus, we propose that IBA57 activates an electron transfer pathway required to reductively couple two [2Fe-2S]$^{2+}$ clusters to form a [4Fe-4S]$^{2+}$ cluster. This step needs to be addressed at a molecular level to accept this model, structurally characterizing both the interaction among ISCA1, ISCA2 and IBA57 and the electron transfer pathway with the electron donor FDX2. To date, structural information are only available on isolated IBA57, whose crystal structure has been solved by us, showing that Cys 230 is highly exposed to the solvent, in agreement with its role, in the heterodimeric complex, of ligand of the [2Fe-2S] cluster bridged between ISCA2 and IBA57 [127]. The IBA57 structure and NMR interaction data also showed that tetrahydrofolate derivatives are not substrates of IBA57, at variance of what it was found in a bacterial structurally homologue of IBA57 (YgfZ). This result has been recently confirmed by functional studies in yeast that showed that yeast Iba57 does not exploit folate for its function [128]. A structural docking model of the [2Fe-2S] ISCA2-IBA57 complex [129] showed that the complex is organized in a dimer of dimers, where ISCA2 forms the homodimerization core interface (Fig. 3B). The [2Fe-2S] cluster is out of the ISCA2 core and it is shared with IBA57 in the dimer of dimers. NMR and gel filtration data indicated the presence of an equilibrium between the dimer of dimers and the [2Fe-2S] ISCA2-IBA57 heterodimer (Fig. 3B). This structural arrangement of dimer of dimers might provide a first hint on how the ternary ISCA1-ISCA2-IBA57 complex is formed. The replacement of one of a ISCA2-IBA57 subunit of the dimer of dimers with a ISCA1-ISCA2 unit would indeed generate a ternary complex containing an ISCA1-ISCA2 unit able to bind a [2Fe-2S] cluster at its interface and an ISCA2-ISCA57 unit also to bind a [2Fe-2S] cluster at its interface (Fig. 3B). This structural module with two bound [2Fe-2S] clusters would be perfectly suitable to assemble a [4Fe-4S] cluster once two electrons are provided by FDX2 (Fig. 3B).

3.4. *Mitochondrial ISC assembly machinery: Dedicated ISC accessory proteins for [4Fe-4S] cluster insertion into mitochondrial target apo proteins*

Accessory proteins of the mitochondrial ISC assembly machinery drive the transfer and insertion of [4Fe-4S] clusters into mitochondrial target apo proteins. Among them, the best-characterized example via NMR is the NFU1 protein. NFU1 is necessary for the biogenesis of some mitochondrial [4Fe-4S] proteins, which are the respiratory complexes I and II [109,110], lipoyl synthase (LIAS) [110,130] and the mitoribosome assembly factor METTL17 [113]. NFU1 is formed by two folded domains connected by a flexible linker. The C-terminal domain (CTD) is highly conserved in the Nfu protein family, while N-terminal domain (NTD) is less conserved. The solution NMR structures of the single CTD and NTD are available [131] and showed that the conserved metal biding CXXC motif of CTD is positioned on a flexible loop (Fig. 3C) [115,131]. NMR, analytical gel filtration and SAXS data showed that full-length apo NFU1 is monomeric and assumes a dumbbell-shaped structure with the two domains not fully independent (Fig. 3C). NMR data provided information that allow us to build a structural docking model of a compact state of apo NFU1. In this structural model, the metal-binding CXXC motif of CTD can be still involved in Fe/S cluster binding as it is fully exposed to the solvent [115]. NMR data also showed that, upon [4Fe-4S]$^{2+}$ cluster binding, NFU1 forms a homodimer in which the cluster bridges two CTDs and is coordinated by two CXXC motifs. Although no residues of the N-domain are directly involved in coordinating the cluster, the presence of the N-domian is important to stabilize cluster binding. Paramagnetic NMR on [4Fe-4S]$^{2+}$ NFU1 dimer showed that the cluster binding site is easily reached by small molecule ligands such as DTT and GSH, which are able indeed to bind to the cluster likely displacing the highly solvent exposed Cys 213 of NFU1 [115]. This coordinative plasticity matches with the cluster trafficking role of NFU1. Indeed, NFU1 is expected to receive the [4Fe-4S] cluster assembled on ISCA1-ISCA2 complex and insert it into target apo proteins.

A NMR-based study recently proposed the molecular events occurring when a [4Fe-4S] cluster need to be inserted into mitochondrial target apo proteins via ISCA1, ISCA2 and NFU1 proteins [132]. ISCA1 is able to individually form complex with both NFU1 and ISCA2. On the contrary, NFU1 and ISCA2 do not form a complex. Upon mixing the three proteins, a transient ISCA1-ISCA2-NFU1 ternary complex is formed. These results indicate that ISCA1 promotes the interaction between the two not interacting NFU1 and ISCA2 proteins. The synergy of paramagnetic and diamagnetic NMR studies defined that ISCA1 specifically interacts with CTD of NFU1 (NTD is not involved in the interaction). This interaction drives the transfer of the [4Fe-4S] cluster from the [4Fe-4S] cluster assembly site on ISCA1-ISCA2 complex to a [4Fe-4S] cluster-binding site shared by ISCA1 and NFU1. This process occurs via the formation of the ISCA1-ISCA2-NFU1 ternary complex, which is transient and evolves, indeed, to form the [4Fe-4S] ISCA1-NFU1 complex upon the release of apo ISCA2 (Fig. 3C). In such a way, the [4Fe-4S] cluster transfer from the ISCA1-ISCA2 complex to NFU1-ISCA1 complex is strictly and specifically controlled and drives the [4Fe-4S] cluster insertion to those target apo proteins that specifically require NFU1 for their maturation (Fig. 3C). Proteomics data in HeLa cells support this model showing the ability of ISCA1 to form a complex with both ISCA2 and NFU1 proteins and that of ISCA2 to complex ISCA1, but not NFU1 [118]. Finally, a site-directed mutagenesis/spectroscopic (NMR and UV-vis) combined approach indicated that the [4Fe-4S]$^{2+}$ cluster in both ISCA1-ISCA2-NFU1 and ISCA1-NFU1 complexes is coordinated by the CXXC motif of NFU1 and by Cys57, and either Cys121 or Cys123 of ISCA1 [133].

A synergistic approach that exploited SEC-SAXS and high-resolution NMR allow us to present the structural models of apo complexes formed by ISCA1, ISCA2 and NFU1 proteins [133]. These models revealed that the structural plasticity of the two domains of NFU1 observed when they interact with different protein partners is the crucial molecular factor allowing a safe and regulated transfer of the [4Fe-4S]$^{2+}$ cluster from the ISCA1-ISCA2 complex to the ISCA1-NFU1 complex. Two conformations of apo NFU1 (extended and compact) were observed when NFU1 is complexed with ISCA1-ISCA2 or with ISCA1 (Fig. 3C). Specifically, in the ternary ISCA1-ISCA2-NFU1 complex, NFU1 assumes an extended conformation where NTD of NFU1 is released in solution (Fig. 3C). The extended conformation of NFU1 in the ternary complex is caused by the position of the ISCA2 subunit, which does not allow, indeed, NTD of NFU1 to assume the compact state. On the contrary, NFU1 assumes a compact conformation in the ISCA1-NFU1 complex, since, upon ISCA2 release, NTD of NFU1 can go spatially close to CTD of NFU1 swapping ISCA2 (Fig. 3C). ISCA1 assumes the same position found in both ISCA1-ISCA2-NFU1 and ISCA1-NFU1 complexes interacting with CTD of NFU1. These data suggest that NTD of NFU1 modulates [4Fe-4S]$^{2+}$ cluster transfer, i.e.: the structural proximity between NTD and CTD observed in

the compact conformation of NFU1 does not allow $[4Fe\text{-}4S]^{2+}$ cluster transfer and its reception from donors, while this transfer is possible in the extended NFU1 conformation only (Fig. 3C). This role of NTD of NFU1 in protecting [4Fe-4S] cluster from its trafficking agrees with the finding that a quantitative $[4Fe\text{-}4S]^{2+}$ cluster binding to CTD was obtained only in the presence of NTD [115].

The last step of the biogenesis of mitochondrial [4Fe-4S] target proteins consists in the insertion of the [4Fe-4S] cluster in their cluster binding sites. Experimental data monitoring the [4Fe-4S] cluster transfer between NFU1 and a mitochondrial apo target protein were provided by solution NMR. The first example consists in [4Fe-4S] cluster delivery to mitochondrial apo aconitase. Solution NMR data suggested that an oligomeric [4Fe-4S] NFU1 state interacts with apo aconitase, and then the formed monomeric apo NFU1 is no longer able to interact with [4Fe-4S] aconitase [131]. Another and deeper NMR investigation of the mechanism of [4Fe-4S] cluster insertion into target apo proteins involved human lipoyl synthase (LIAS), which belongs to the radical S-adenosylmethionine (SAM) superfamily [134,135]. LIAS has two [4Fe-4S] clusters [136,137], one (named FeS_{RS}) is distinctive of all radical SAM enzymes [138], and the other (named FeS_{aux}) makes available two sulfur atoms to biosynthesize the lipoyl cofactor [139]. In vivo studies revealed that NFU1 is protein partner of LIAS [140] and is fundamental for cluster insertion into LIAS [141]. Solution NMR showed that a LIAS form mostly populating a $[4Fe\text{-}4S]^{2+}$ cluster at its FeS_{aux} site ($LIAS_{aux}$, hereafter) forms a stable heterodimeric complex with apo NFU1 [142]. ITC data confirmed this tight interaction resulting with a dissociation constant of 0.7 ± 0.2 μM [143]. The NMR data showed that the interaction surface of NFU1 with LIAS comprises the two helices of CTD encasing the cluster binding CXXC site. This region is essentially the same interface of NFU1 found in the interaction of NFU1 with ISCA1. NMR data coupled with analytical gel filtration also showed that, once $LIAS_{aux}$ is added to apo or [4Fe-4S] ISCA1-NFU1 complex, it displaces ISCA1 to form a dimeric apo or [4Fe-4S] NFU1-$LIAS_{aux\ complex}$, with no detection of a stable ISCA1-NFU1-$LIAS_{aux}$ ternary complex [142]. Thus, [4Fe-4S] cluster insertion into $LIAS_{aux}$ to generate matured LIAS with cluster-loaded at the RS site occurs with the displacement of ISCA1 (Fig. 3C) [142]. CTD of NFU1 interacts with LIAS stronger than with ISCA1, thus replacing ISCA1 in the heterocomplex by competition for the same binding surface [142]. In conclusion, solution NMR data were able to dissect the NFU1-dependent mechanism of maturation of LIAS (Fig. 3C). An affinity gradient of the interaction of the C-domain of NFU1 that increases from ISCA1 to LIAS directs the [4Fe-4S] cluster to its final destination. Recent biochemical data showed that NFU1 efficiently restore FeS_{aux} of LIAS in its enzymatic cycle [143], thus suggesting that the mechanism we proposed can also be active in cluster insertion into the FeS_{aux} site of LIAS. As final consideration, it is remarkable that NTD and CTD domains in NfuA, the *E. coli* homologue of human NFU1, work differently. Indeed, it has been found that NTD of NfuA is essential for recognizing *E. coli* lipoyl synthase (LipA) by tightly interacting with it, while the CTD of NfuA, which binds a [4Fe-4S] cluster like human NFU1, does not interact with LipA [144]. This different behaviour, although at first glance surprising, can be rationalized considering that the structure of the two N-domains is profoundly different [145], providing us an important lesson on how similar modular domain architectures not always can bring to extrapolate a general mechanism applicable from one organism to another (in particular when going from bacteria, archeae to mammals), but that the protein surface is the crucial factor in selecting protein interaction partners.

3.5. Mitochondrial ISC assembly machinery: potential alternative pathways operating in the biogenesis of mitochondrial [4Fe-4S] proteins

An alternative pathway in the maturation of mitochondrial [4Fe-4S] proteins, which was proposed based on exclusive in vitro data, envisages [4Fe-4S] cluster assembly on ISCU2 and its transfer to apo NFU1. It has been observed that a [4Fe-4S] cluster can be assembled on ISCU2 at the core ISC complex once iron and cysteine are provided, and that this cluster can be then transferred to NFU1 [146] as well as to aconitase to produce an active enzyme [146,147]. The interaction and the cluster transfer between [4Fe-4S] ISCU2 and apo NFU1 have been characterized in vitro by NMR. $^{1}H\text{-}^{15}N$ TROSY HSQC experiments reveal specific interactions between two α-helices of CTD of NFU1 and the Fe/S cluster binding site of ISCU2 [146]. These NMR data combined with SAXS data generated a docking model of the complex. $^{1}H\text{-}^{15}N$ TROSY HSQC experiments also showed a selectivity of the cluster transfer process, which exclusively occurs with a [4Fe-4S] cluster but not with a [2Fe-2S] cluster. However, the described in vitro reaction experiments have been questioned as a non-physiological process [95,148]. The assembly of the [4Fe-4S] cluster on ISCU2 requires indeed a high concentration of the no physiological reducing agent DTT.

Another alternative pathway possibly operating in the maturation of mitochondrial [4Fe-4S] proteins includes the function of BOLA3 in assembling [4Fe-4S] clusters on NFU1. Human BOLA3 protein has been, indeed, implicated to act in the mitochondrial ISC assembly machinery not only once complexed with GLRX5, but also interacting with NFU1 to generate the lipoyl cofactor [149]. The tight interaction ($K_d = 3 \pm 0.8$ μM range) detected by microscale thermophoresis between apo/holo NFU1 and BOLA3 suggested that BOLA3 complexed with NFU1 is the species required to insert the [4Fe-4S] cluster into LIAS [19]. However, NMR studies ruled out this model as BOLA3 was shown to do not interact with NFU1 either in its apo or $[4Fe\text{-}4S]^{2+}$ form. This is consistent with ITC data that showed a very weak binding between apo NFU1 and BOLA3 [114]. Moreover, once BOLA3 was included in NFU1-LIAS activity assays no additional effect on turnover was observed, as well as size exclusion chromatography experiments showed that BOLA3 is not tightly bound to LIAS [143]. Overall, these in vitro findings exclude that BOLA3 directly operates in the cluster insertion pathway into LIAS. However, the still open question is why a similar reduced lipoate synthesis is observed in pathogenic NFU1 or BOLA3 mutants [109,141]. On this aspect, solution NMR data suggested that an alternative BOLA3-dependent pathway, which forms a [4Fe-4S] cluster in NFU1 and is independent by ISCA1-ISCA2-IBA57 pathway, might be operative [115]. The data showed indeed that a $[4Fe\text{-}4S]^{2+}$ cluster can be formed on dimeric NFU1 once the $[2Fe\text{-}2S]^{2+}$ GLRX5-BOLA3 complex is added to monomeric apo NFU1 in the presence of DTT. Although the reaction is not very efficient, likely because DTT is not the physiological electron donor, the reaction is specific as it does not occur once $[2Fe\text{-}2S]^{2+}$ GLRX5 is mixed with apo NFU1 only [115]. Thus, this [4Fe-4S] cluster assembly pathway on NFU1 is triggered only once both GLRX5 and BOLA3 are present. On the other hand, the physiological relevance of this pathway needs to be fully demonstrated, as well as a physiological reductant needs to be identified.

3.6. CIA machinery: electron transfer to assemble a [4Fe-4S] cluster by the NDOR1-anamorsin complex

In its first stages of action, the CIA machinery, operative in the cytoplasm, requires electrons to assemble a $[4Fe\text{-}4S]^{2+}$ cluster following a mechanism similar to that found in mitochondria where two $[2Fe\text{-}2S]^{2+}$ clusters are reductively coupled. This [4Fe-4S] cluster assembly mechanism is actually largely debated and two distinct models have been proposed by Lill's [150,151] and Rouault's [152,153] groups, respectively. Both models require electrons to assemble a [4Fe-4S] cluster on a scaffold protein. While in the Rouault's model the electron donor was still not identified, in the Lill's model two human cytosolic proteins, i.e. NADPH-dependent diflavin oxidoreductase 1 (NDOR1) and anamorsin, were suggested to be the source of electrons required for assembling a $[4Fe\text{-}4S]^{2+}$ cluster in the cytosol [154,155].

NMR studies significantly contributed to the investigation of the electron transfer process required to assemble the cytosolic [4Fe-4S] cluster. By solution NMR, we characterized the structure of anamorsin, showing that it is formed by a N-terminal well-folded domain

connected by a long unstructured and flexible linker to a largely unstructured, C-terminal CIAPIN1 domain [156,157] (Fig. 4). The CIAPIN1 domain contains two highly conserved cysteine motifs present in several eukaryotic proteins, i.e. CX_8CX_2CXC and $CX_2CX_7CX_2C$ [158]. Combining paramagnetic NMR, UV/vis, EPR, Mössbauer and MS techniques, we showed that each motif independently coordinates a [2Fe-2S] cluster (Fig. 4) [156,159]. Other works showed that anamorsin homologues belonging to the eukaryotic CIAPIN1 protein family bind [4Fe-4S] or [2Fe-2S] clusters depending on the purification procedures used to isolate the holo species [160–163]. Our recent studies on the Fe/S binding properties of human anamorsin, performed by *in cellulo* Mössbauer and *in cellulo* EPR spectroscopies, have helped to make clarity showing that no [4Fe-4S] clusters were detected to be bound to anamorsin but two [2Fe-2S] clusters were bound at both motifs of anamorsin, consistently with the model that $[2Fe\text{-}2S]_2$-anamorsin is the physiologically species [15]. This finding agrees with in vivo data on yeast Dre2, which showed that its maturation does not require any member of the CIA machinery that is known to be involved in the maturation of cytosolic [4Fe-4S] proteins [155].

Solution NMR also contributed to define the molecular grounds of the interaction between NDOR1 and anamorsin as well as provided information on the electron transfer between them. The two proteins form a stable complex which, first, drives the transfer of two electrons from NADPH to FMN moiety of NDOR1 to form the hydroquinone state of FMN ($FMNH_2$, Fig. 4) [157]. Then, the electrons are sequentially transferred to the [2Fe-2S] cluster bound to the CX_8CX_2CXC motif of anamorsin to form the reduced $[2Fe\text{-}2S]^+$ cluster, but they are not transferred to the other [2Fe-2S] cluster of anamorsin bound to the $CX_2CX_7CX_2C$ motif [157,159] (Fig. 4). A completely unstructured region of anamorsin, located in the long linker of anamorsin, interacts with a α-helical patch of the FMN-binding domain of NDOR1 (Fig. 4). On the contrary, the well-folded N-terminal domain of anamorsin does not take part to the complex formation (Fig. 4). It was also shown by solution NMR that the [2Fe-2S] cluster bound to the CX_8CX_2CXC motif and FMN transiently interact via an electrostatic attraction between a negatively charged region surrounding FMN and a positively charged region surrounding the [2Fe-2S] cluster [157]. Overall, the NMR data define a stable complex thanks to the tight interaction between regions that are far from the redox cofactors of anamorsin and NDOR1, and indicate a structural dynamicity of the interaction between the redox cofactors, which indeed transiently and weakly interact with each other.

Very recently, we identified a molecular target of the electron transfer pathway activated by the NADPH-NDOR1-anamorsin complex formation. This is the cytosolic protein NUBP1, which is a component of the CIA machinery [164]. NUBP1 contains a [4Fe-4S] cluster at its N-terminal domain tightly bound via a conserved $CX_{13}CX_2CX_5C$ motif [22,164,165]. The assembly of this cluster requires two electrons to reductively couple two $[2Fe\text{-}2S]^{2+}$ clusters (Fig. 4) [166]. We showed, via a combination of paramagnetic NMR, EPR and analytical SEC techniques, that a complex, formed by two molecules of $[2Fe\text{-}2S]^{+}_2$ anamorsin and one molecule of dimeric $[2Fe\text{-}2S]^{2+}_2$-$GLRX3_2$, synergically provides two $[2Fe\text{-}2S]^{2+}$ clusters from GLRX3 and two electrons from the [2Fe-2S] cluster bound to the CX_8CX_2CXC motif of anamorsin to assemble the $[4Fe\text{-}4S]^{2+}$ cluster on the N-terminal cluster binding site of NUBP1 (Fig. 5A) [166]. This assembly process agrees with the functional role of GLRX3 proposed in the CIA machinery. Indeed, GLRX3 is a cytosolic monothiol glutaredoxin able to bind, in a labile manner, two $[2Fe\text{-}2S]^{2+}$ clusters that can be delivered in the early steps of the CIA machinery [167]. The protein dimerizes upon binding of two bridged $[2Fe\text{-}2S]^{2+}$ clusters as shown in Fig. 5A [22,168,169] and it has been shown in vitro to act as a [2Fe-2S] cluster chaperone versus various proteins [170,171], including NUBP1 [22]. In particular, while the [4Fe-4S] cluster tightly bound to the N-terminal site of NUBP1 behaves like a final cytosolic acceptor of [4Fe-4S] clusters assembled by GLRX3-anamorsin complex (as described above), the $[4Fe\text{-}4S]^{2+}$ cluster bound at the C-terminal motif is labile [22,165]. The biogenesis of N-terminal [4Fe-4S] cluster in the yeast homologue of NUBP1 was shown to require the homologue of anamorsin, Dre2 [155], but does not use proteins working later in the CIA machinery [172]. This behaviour is markedly different from what occurs for the biogenesis of the majority of cytosolic [4Fe-4S] proteins that, indeed, require both early and late acting components of the CIA machinery [20,167]. These findings fit well with the maturation mechanism we found for the N-terminal [4Fe-4S] cluster of NUBP1.

NMR studies have also shown that GSH can activate the assembly of a $[4Fe\text{-}4S]^{2+}$ cluster at the C-terminal cluster binding site of NUBP1, although not being very efficient [22]. This process proceeds only if the [4Fe-4S] cluster is present at the N-terminal site, suggesting a cooperativity effect between the N- and the C-terminal sites to drive the formation of a [4Fe-4S] cluster at the C-terminal site. The same is not true for the assembly of the [4Fe-4S] cluster at the N-terminal site, which, indeed, can assemble independently by the presence of a [4Fe-4S] cluster at the C-terminal site. A possible model explaining this synergic effect is that the N-terminal [4Fe-4S] cluster is reduced by the

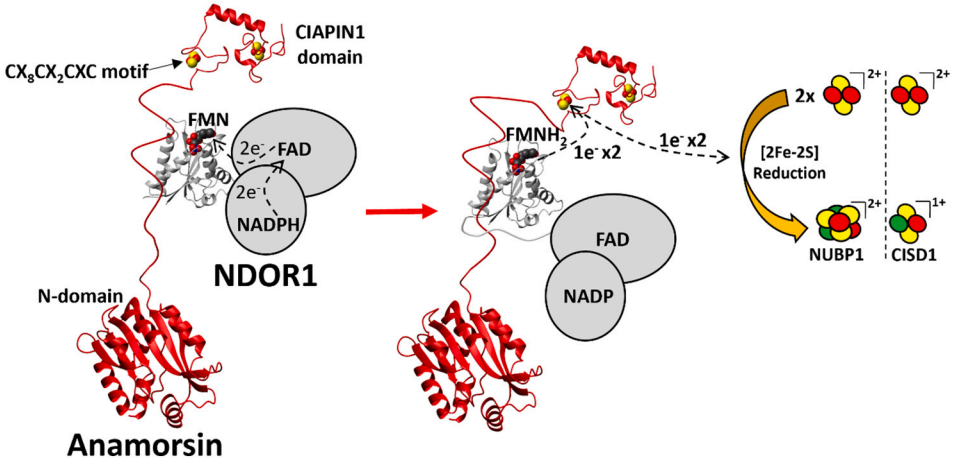

Fig. 4. Electron transfer pathway guiding [4Fe-4S] cluster assembly in the cytosol based on integrated structural biology data. Electrons are transferred from NADPH via the FAD- and FMN-containing NDOR1 to the [2Fe-2S] cluster bound to the CX_8CX_2CXC motif of anamorsin. $[2Fe\text{-}2S]^{2+}$ cluster reduction can then generate a $[4Fe\text{-}4S]^{2+}$ cluster on NUBP1 or a reduced $[2Fe\text{-}2S]^{2+}$ cluster on CISD1. Red colors were used to highlight proteins and pathways that have been characterized through solution NMR. Structural models of human proteins, solved by X-ray crystallography or solution NMR, were reported. [2Fe-2S] and [4Fe-4S] clusters were represented as red and green (for Fe^{3+} and Fe^{2+}, respectively) and yellow (for S) spheres. PDB IDs are: NDOR1(FMN-binding domain)-4H2D and N-domain of anamorsin-2LD4.

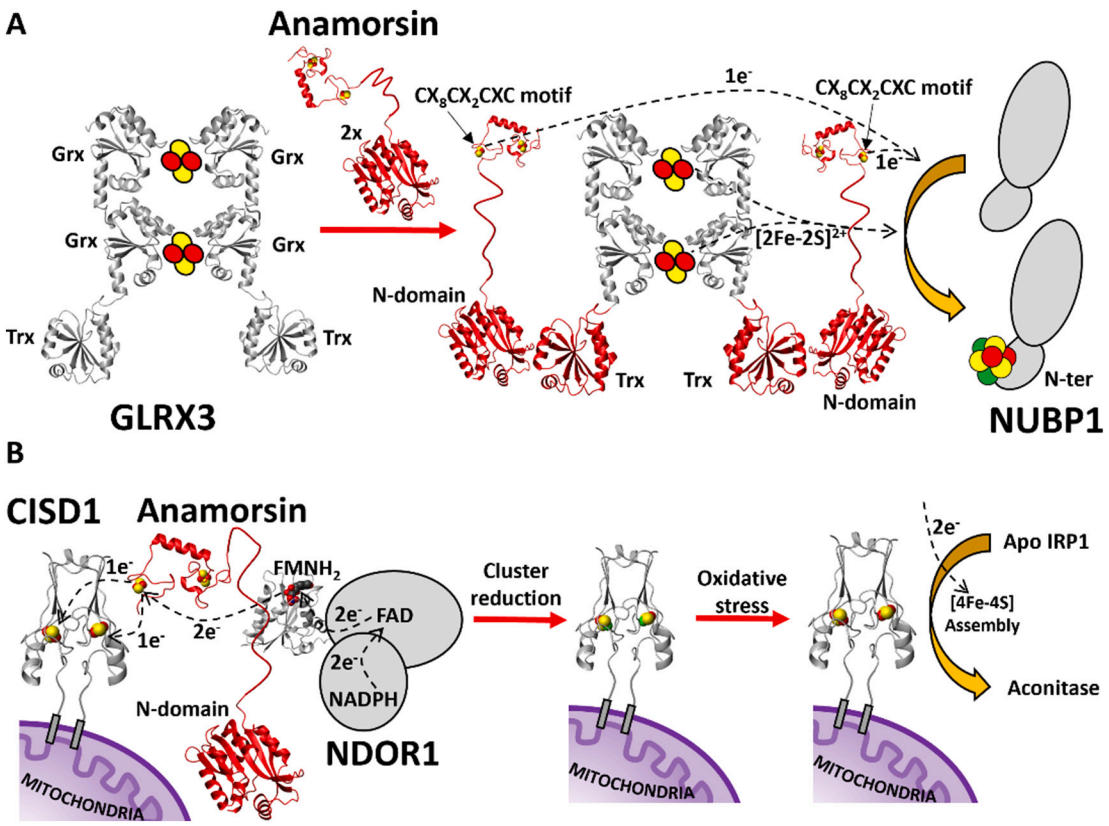

Fig. 5. Molecular model of cytosolic [4Fe-4S] cluster assembly on NUBP1 and IRP1 based on integrated structural biology data. A) $[2Fe\text{-}2S]_2^{2+}$ anamorsin and dimeric $[2Fe\text{-}2S]_2^{2+}$-$GLRX3_2$ orchestrate the assembly of a $[4Fe\text{-}4S]^{2+}$ cluster on the N-terminal cluster binding site of NUBP1. B) [2Fe-2S] cluster reduction of CISD1 mediated by the NDOR1-anamorsin complex and $[4Fe\text{-}4S]^{2+}$ cluster assembly on cytosolic apo IRP1 under oxidative stress. Red colour was used to highlight proteins and pathways that have been characterized through solution NMR. Structural models of human proteins, solved by X-ray crystallography or solution NMR, were reported. [2Fe-2S] and [4Fe-4S] clusters were represented as red and green (for Fe^{3+} and Fe^{2+}, respectively) and yellow (for S) spheres. PDB IDs are: GLRX3(Trx domain)-2WZ9, GLRX3(first Grx domain)-3ZYW, GLRX3(second Grx domain)-2YAN, and CISD1-3REE.

NDOR1-anamorsin complex, and the received electrons are then sequentially supplied to the C-terminal site to assemble a [4Fe-4S] cluster on it. This possible mechanism is intriguing but still needs to be characterized.

3.7. CIA machinery: other potential electron transfers pathways driven by the NDOR1-anamorsin complex

CISD1 belongs to the NEET protein family, which is a class of protein able to bind two [2Fe-2S] clusters coordinated by a unique 3 Cys:1 His coordination motif [173]. NMR spectroscopy complemented by UV–vis spectroscopy showed that the NDOR1-anamorsin complex can act as reducing agent of the [2Fe-2S] clusters bound to CISD1 via the formation of a transient complex that approaches each [2Fe-2S] cluster of CIDS1 to the redox-active [2Fe-2S] cluster of anamorsin, i.e. the one bound by the CX_8CX_2CXC motif (Fig. 5B) [174]. This specific interaction exclusively involves anamorsin and CISD1, but not NDOR1. The physiological role of this electron transfer pathway is still unknown, but a potential function can be proposed by NMR studies. They showed that the holo form of CISD1 is well folded, while the apo form is highly disordered. Thus, the two forms can cycle just by insertion/transfer of the [2Fe-2S] cluster [175]. Moreover, it was showed that an appropriate redox state of the [2Fe-2S] clusters bound to CISD1 is crucial to transfer them from CISD1 to a target [2Fe-2S]-receiving protein [176–178]. Once the clusters are in the reduced $[2Fe\text{-}2S]^+$ state, they are not kinetically labile and are not released, while, once they are in the oxidized $[2Fe\text{-}2S]^{2+}$ state, they are labile and transferable to an apo protein [178–180]. Thus, cluster reduction of CISD1 driven by the NDOR1-anamorsin complex might act as a regulatory mechanism that controls the cluster transfer properties of CISD1. In this model, under oxidative stress conditions, in which the NDOR1-anamorsin electron pumping system might be impaired [181] as the solvent-exposed [2Fe-2S] clusters of anamorsin are damaged by the oxidative environment [32], the [2Fe-2S] clusters of CISD1, which were found resistant to NO and H_2O_2, turn out to be oxidized/labile and able to be released for repairing cytosolic apo IRP1 (Fig. 5B). The latter, once produced by oxidative stress [175], has been shown indeed to be converted to [4Fe-4S] aconitase by CISD1 by direct Fe/S transfer in the presence of DTT as reductant that provides two electrons required to assemble the [4Fe-4S] cluster (Fig. 5B). Upon the reduction of oxidative stress conditions, the NDOR1-anamorsin complex of the CIA machinery is re-activated and able to reduce the [2Fe-2S] clusters of CISD1 thus stopping the [2Fe-2S] cluster transfer activity of CISD1. In such model, the CIA machinery only operates to mature [4Fe-4S] proteins under cellular conditions with no oxidative stress [174,175,179]. The here described [2Fe-2S] cluster transfer role of CISD1, as well as of its homologous CISD2, was proposed to be active when GLRX3 is depleted in human cells, thus possibly representing a cellular mechanism bypassing GLRX3-dependent cluster transfer pathway [182]. GLRX3 depletion determines, indeed, modest deficiencies of cytosolic Fe/S cluster enzymes [169], supporting that the [2Fe-2S] cluster transfer function of GLRX3 might be replaced by the NEET proteins.

3.8. CIA machinery: [2Fe-2S] cluster insertion into anamorsin

Solution NMR provided the first evidence of a mechanism inserting [2Fe-2S] clusters into both Fe/S cluster binding motifs of anamorsin by $[2Fe\text{-}2S]_2$-$GLRX3_2$ [170]. These two proteins were previously shown to

be protein partners in vivo and involved in the CIA machinery [155,169,183]. NMR data showed that, when $[2Fe\text{-}2S]_2$-$GLRX3_2$ was mixed with apo anamorsin, both [2Fe-2S] clusters of GLRX3 were transferred into the two cluster binding sites of anamorsin. Moreover, solution NMR showed that the N-terminal domain of GLRX3 tightly interacts with the N-terminal domain of anamorsin and that this interaction is required to activate the cluster transfer from the two couples of Grx domains of dimeric GLRX3 sharing a [2Fe-2S] cluster to both Fe/S cluster motifs of the CIAPIN1 domain of anamorsin (Fig. 6), which are transiently interacting each other. The NMR data once integrated with protein-protein docking also describe how the N-terminal domains of GLRX3 and anamorsin reciprocally interact and showed that the linker of anamorsin contribute to the stabilization of the protein-protein complex. This study defined for the first time a molecular function for the N-terminal domains of GLRX3 and anamorsin.

After cluster transfer from GLRX3 to anamorsin occurred, a stable heterodimeric complex, formed by a molecule of apo GLRX3 and a molecule of $[2Fe\text{-}2S]_2$ anamorsin, was obtained. This complex, is tightly stabilized by the interaction between the N-terminal domains and the linker of anamorsin. On the contrary, the other domains of anamorsin and GLRX3 (i.e. CIAPIN1 domain and the Grx domains, respectively) do not form a stable interaction. The apo GLRX3-$[2Fe\text{-}2S]_2$ anamorsin complex thus needs to be released in order to form the NDOR1-$[2Fe\text{-}2S]_2$ anamorsin complex which provides electrons to assemble cytosolic [4Fe-4S] clusters (Fig. 6). Considering that, by solution NMR, we found that the linker of anamorsin is a structural determinant of the tight interaction with NDOR1 [157], we can hypothesize that the linker of anamorsin releases its interaction with GLRX3 in the apo GLRX3-$[2Fe\text{-}2S]_2$-anamorsin complex to promote its tighter interaction with NDOR1. As final consequence of this process, the apo GLRX3-$[2Fe\text{-}2S]_2$-anamorsin complex evolves to the NDOR1-$[2Fe\text{-}2S]_2$-anamorsin complex. In such molecular model, the linker of anamorsin thus properly modulates its interactions with GLRX3 and NDOR1 protein partners to promote the formation of the mature redox-competent state of anamorsin, which can receive electrons from NDOR1. This molecular model still requires to be experimentally validated.

Another well-characterized protein partner of GLRX3 is BOLA2 [184], which is a cytosolic protein of the BolA protein family [105,168,185]. BOLA2 has been associated with iron homeostasis in humans responding to changes in cellular iron availability and has a role in protecting against iron deficiency [186,187]. NMR and biochemical studies showed that a heterotrimeric complex formed by a GLRX3 molecule and two BOLA2 molecules stably coordinates two bridged [2Fe-2S] clusters (Fig. 6) [18,168]. The data indicate that the trimeric complex can be formed between the apo proteins with an affinity of 25 ± 15 μM (Fig. 6), and that the Fe/S cluster binding region of BOLA2 [168], interacts with the regions of each Grx domain of GLRX3 involved in $[2Fe\text{-}2S]^{2+}$ cluster binding, while Trx domain of GLRX3 is not involved in such interaction [18]. Upon $[2Fe\text{-}2S]^{2+}$ cluster binding, each cluster in the GLRX3-$BOLA2_2$ heterotrimeric complex is coordinated by the conserved cysteine of Grx domain, by a glutathione bound to Grx domain and by a conserved histidine residue in BOLA2. The fourth ligand was not yet clearly recognized. When apo BOLA2 is mixed with $[2Fe\text{-}2S]_2$ $GLRX3_2$, a heterotrimeric GLRX3-$BOLA2_2$ complex, structurally similar to that formed in the apo heterotrimeric complex, but containing bridged $[2Fe\text{-}2S]^{2+}$ cluster(s), is preferentially formed, likewise

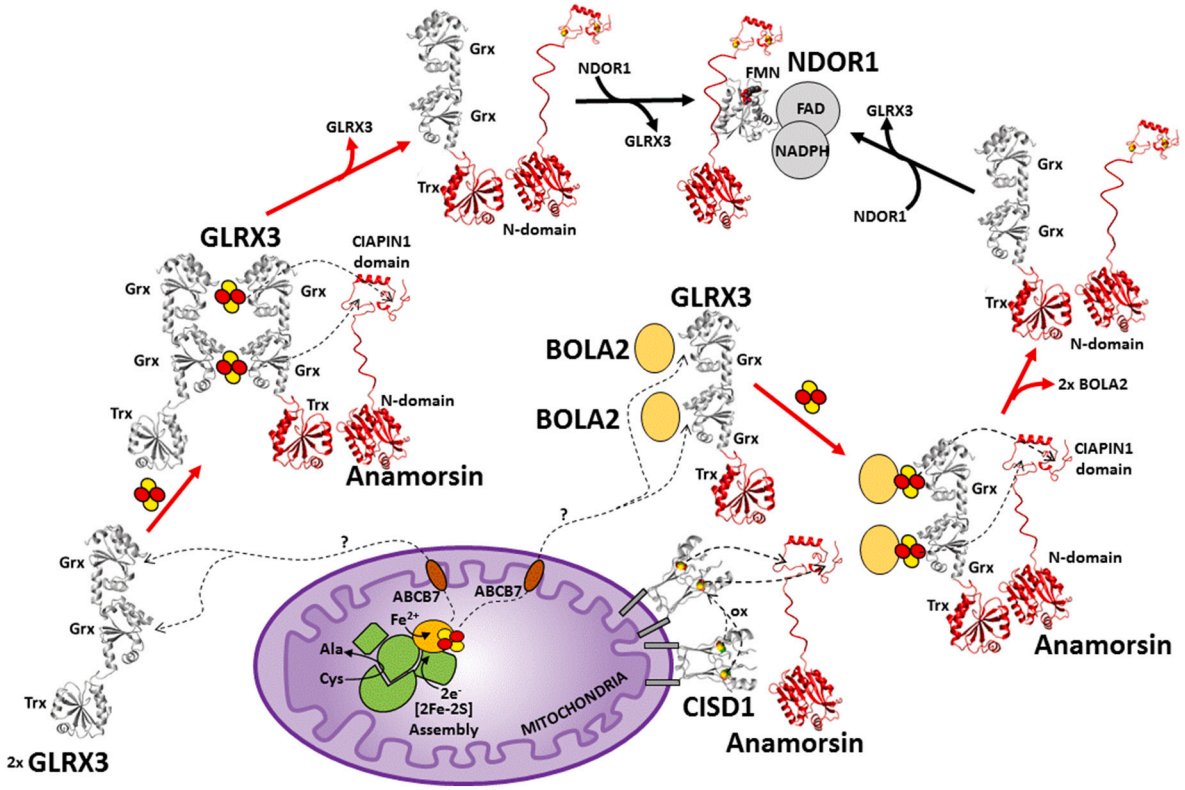

Fig. 6. [2Fe-2S] cluster insertion into anamorsin based on integrated structural biology data. Apo GLRX3 and apo GLRX3-BOLA2 complex binds $[2Fe\text{-}2S]^{2+}$ clusters to form $[2Fe\text{-}2S]_2^{2+}$-$GLRX3_2$ and $[2Fe\text{-}2S]_2^{2+}$-GLRX3-$BOLA2_2$, respectively. The latter transfer their two $[2Fe\text{-}2S]^{2+}$ clusters to the CIAPIN1 domain of anamorsin. The formed GLRX3-$[2Fe\text{-}2S]_2^{2+}$ anamorsin complexes interact with NDOR1 to form the matured NDOR1-anamorsin complex, which can perform its electron transfer function. ABCB7 exports an unknown, sulfur-containing molecule to the cytosol, which was proposed to be required for Fe/S cluster insertion into GLRX3 [188]. As an alternative pathway, anamorsin can be maturated by CISD1, which, upon oxidation of its two [2Fe-2S] clusters (ox), transfer the oxidized clusters to anamorsin. Red colour was used to highlight proteins and pathways that have been characterized through solution NMR. Structural models of human proteins, solved by X-ray crystallography or solution NMR, were reported. [2Fe-2S] clusters were represented as red and green (for Fe^{3+} and Fe^{2+}, respectively) and yellow (for S) spheres. PDB-IDs already mentioned in Figs. 4 and 5.

to what was found in the mitochondrial homologous GLRX5, BOLA1 and BOLA3 proteins (see above).

The $[2Fe\text{-}2S]_2$-GLRX3-$BOLA2_2$ quantitatively transfers in vitro its two [2Fe-2S] clusters to apo anamorsin to obtain $[2Fe\text{-}2S]_2$-anamorsin [18] through the same mechanism described above for $[2Fe\text{-}2S]_2$ $GLRX3_2$ (Fig. 6) [170]. Subsequent in vivo studies showed that this process can also occur in mammalian cells, thus supporting that $[2Fe\text{-}2S]_2$-GLRX3-$BOLA2_2$ works as a [2Fe-2S] cluster chaperone [182]. The cellular studies also showed that high iron concentrations increase the cellular abundance of the GLRX3-BOLA2 complex and that GLRX3-GLRX3 homodimeric complex is less stable and transitory species are formed at a cellular level. In a cell, both $[2Fe\text{-}2S]_2$ $GLRX3_2$ and $[2Fe\text{-}2S]_2$-GLRX3-$BOLA2_2$ can play a role in maturing anamorsin. It is possible that both complexes are operative and that the cellular conditions select, between two complexes, the cluster donor of anamorsin. Considering that $[2Fe\text{-}2S]^{2+}$ clusters bound to the GLRX3-$BOLA2_2$ complex is more stable vs. oxidative degradation than the [2Fe-2S] cluster bound to $[2Fe\text{-}2S]_2$ $GLRX3_2$ [168], it is possible that low oxygen cellular conditions vs. oxidative stress is a discriminatory factor between the two anamorsin-maturing complexes.

The NMR data complemented with analytical gel filtration analysis indicate that the heterotrimeric GLRX3-$BOLA2_2$ complex with both bound $[2Fe\text{-}2S]^{2+}$ clusters is preferentially formed when two $[2Fe\text{-}2S]^{2+}$ clusters are inserted in an already pre-formed apo GLRX3-$BOLA2_2$ complex. NMR showed indeed that the same result cannot be reached by adding $[2Fe\text{-}2S]_2$ $GLRX3_2$ to BOLA2, since, in this case just, a mixture of holo GLRX3-$BOLA2_2$ complexes containing just one $[2Fe\text{-}2S]^{2+}$ cluster was obtained. Therefore, it is realistic to propose that the apo GLRX3-$BOLA2_2$ complex receives two $[2Fe\text{-}2S]^{2+}$ clusters from a cluster donor. However, which might be the [2Fe-2S] cluster donor for the latter complex is still a matter of debate in the literature [188–191]. A recent structural work support that the mitochondrial ABC transporter ABCB7 is in charge of transferring [2Fe-2S] clusters assembled by the mitochondrial ISC machinery, thus making [2Fe-2S] cluster available in the cytosol. However, the identification of ABCB7 physiological substrates still requires further functional investigations [192]. A still unknown molecule exported by ABCB7 was shown to be required for the biogenesis of cytosolic-nuclear Fe/S proteins and cellular iron regulation, possibly targeting GLRX3 that acts early in the CIA machinery (Fig. 6) [188]. On the other hand, recent biochemical analysis, performed in cells and in vitro proposed a new view of the cytosolic [2Fe-2S] cluster assembly process, indicating that the iron binding protein PCBP1 and BOLA2 form a complex with glutathione and Fe^{2+} ion bound, which is responsible for the formation of [2Fe-2S] clusters on the BOLA2-GLRX3 complex [193,194]. Spectroscopic and structural evidences, showing the formation of the PCBP1-Fe-GSH-BOLA2 complex as well as its iron donor function to apo GLRX3-BOLA2 complex to assemble the [2Fe-2S] cluster, would be fundamental to validate this model. Moreover, how the sulfide is originated to assemble the [2Fe-2S] cluster in the GLRX3-BOLA2 complex is still elusive.

Another route proposed for anamorsin maturation involves the NEET proteins. By using UV–Vis spectroscopy and electrospray mass spectrometry, it was shown that CISD1 and CISD2 interact with apo anamorsin and transfer to it their [2Fe-2S] clusters, only once oxidized, to obtain mature $[2Fe\text{-}2S]_2$-anamorsin (Fig. 6) [177]. This alternative pathway is supported by the finding that yeast Dre2 is bound in a large fraction to the cytosolic side of the outer membrane of mitochondria, where CISD1 protein is also localized [195].

3.9. CIA machinery: [4Fe-4S] cluster insertion to cytosolic target apo proteins by dedicated CIA accessory proteins

Once the cytosolic [4Fe-4S] cluster is generated, its transfer to apo proteins is specifically mediated by several proteins of the CIA machinery [196]. Among these proteins there is the iron-hydrogenase-like protein NARFL (also known as IOP1 and CIAO3 [197]), which accepts the [4Fe-4S] cluster bridged between the NUBP1-NUBP2 complex (i.e. where a cytosolic [4Fe-4S] cluster is assembled) and delivers it to the CIA targeting complex (CTC), that is formed by CIAO1, CIAO2B and MMS19 proteins [198–204], and to the CIAO1-CIAO2A complex (Fig. 7) [200,205]. Crystal and cyro-EM structures of CTC and of CTC complexed with CTC-target proteins has been recently solved, showing that CIAO2B is central to the complex and connects CIAO1 and MMS19 (Fig. 7) [23]. This structure, however, does not provide a clear picture of how the [4Fe-4S] cluster is inserted in a target apo protein. Concerning the [4Fe-4S] cluster transfer from CIAO3 to the CIAO1-CIAO2A complex, a recent study showed that [4Fe-4S] CIAO3 stably interacts only once a heterodimeric complex between CIAO2A and CIAO1 is formed, while it does not interact with the individual CIAO2A and CIAO1 proteins [206]. This study also demonstrated that the interaction between the three proteins requires the binding of the [4Fe-4S] cluster at the C-terminal motif of CIAO3, while it is independent by the binding of the [4Fe-4S] cluster at the N-terminal site of CIAO3. This is in agreement with the structural role of the C-terminal cluster with respect to that bound to the N-terminus, which is solvent exposed and labile [207].

NMR studies investigated the pathway involving CIAO3 and the CIAO1-CIAO2A complex. The structure of monomeric CIAO2A solved by solution NMR is available (Fig. 7) [208], and two distinct structures of dimeric CIAO2A were reported by X-ray crystallography [208,209]. In a recent NMR study, we showed that CIAO2A is preferentially monomeric in solution and that it binds a [4Fe-4S] cluster only once it is complexed with CIAO1 (Fig. 7) [210]. Specifically, it has been shown that a stable apo heterodimeric complex is formed between CIAO2A and CIAO1, and that, upon [4Fe-4S] cluster binding, it evolves to a complex that contains one CIAO1 molecule and two CIAO2A molecules ([4Fe-4S] CIAO1-$CIAO2A_2$), likely arranged in the dimeric state of the crystal structure able to bind a zinc ion (which mimics the [4Fe-4S] cluster binding [209,210]) by Cys 90 (Fig. 7). At support of the physiological relevance of this complex, it has been found that the [4Fe-4S] cluster bound to [4Fe-4S] CIAO1-$CIAO2A_2$ can be transferred to apo IRP1 to generate aconitase (Fig. 7) [210]. The switch from the apo CIAO1-CIAO2A heterodimeric complex to the [4Fe-4S] CIAO1-$CIAO2A_2$ complex might be caused by the interaction of $[4Fe\text{-}4S]_2$ CIAO3 with the apo CIAO1-CIAO2A heterodimeric complex. A ternary $[4Fe\text{-}4S]_2$ CIAO3-CIAO1-CIAO2A intermediate might be the key element formed to drive [4Fe-4S] cluster transfer from the N-terminal solvent exposed cluster binding site of CIAO3 to that defined by the dimerization of CIAO2A (Fig. 7). The role of the [4Fe-4S] form of CIAO3 in bridging the interaction between the heterodimeric NUBP1-NUBP2 complex and the CTC complex has been recently demonstrated [202], thus supporting that [4Fe-4S] CIAO3 can similarly act in the transfer of the [4Fe-4S] cluster from CIAO3 to CIAO1-CIAO2A complex.

Recent biochemical\spectroscopic studies including NMR contributed to the characterization of the maturation of an ATP-binding cassette (ABC)-ATPase ABCE1 that binds two [4Fe-4S] clusters [211]. The maturation of ABCE1 includes two additional accessory proteins, which form a complex formed by ORAOV1 and YAE1 proteins ('CIA adapter complex' hereafter) [212,213]. The current molecular model suggests that the 'CIA adapter complex' assists the insertion of [4Fe-4S] clusters, received from the CIA targeting complex, into the apo form of ABCE1 (Fig. 7). Recent data showed that ORAOV1 is able to bind a $[4Fe\text{-}4S]^{2+}$ cluster and it is an homodimer in both apo and holo forms, largely composed by α-helical and flexible unstructured regions [211]. Fe/S cluster binding in ORAOV1 is consistent with the presence of a conserved CX_9CX_4C motif and of a conserved Cys 117. Similarly, to isolated ORAOV1, the 'CIA adapter complex', a heterodimer formed by one molecule of ORAOV1 and one of YAE1, is composed by unstructured and α-helical regions, and binds a $[4Fe\text{-}4S]^{2+}$ cluster (Fig. 7). Site-directed mutagenesis coupled with spectroscopic analysis favours a structural model where, in the YAE1-ORAOV1 heterocomplex, the [4Fe-4S] cluster is exclusively bound to the conserved cluster-binding motif of ORAOV1. Indeed, YAE1 has not a metal-binding consensus motif.

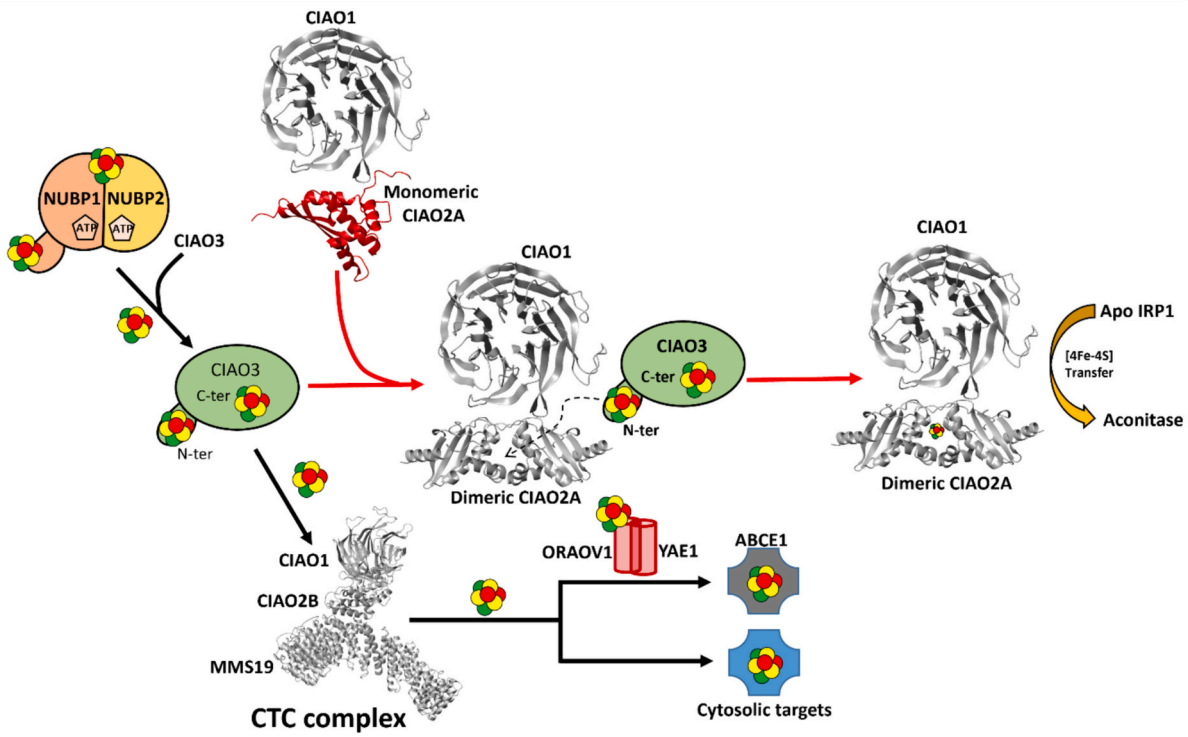

Fig. 7. Molecular model of [4Fe-4S] cluster insertion to cytosolic target apo proteins by dedicated CIA accessory proteins based on integrated structural biology data. The NUBP1-NUBP2 complex assembles a $[4Fe\text{-}4S]^{2+}$ cluster bridged between the two proteins. This cluster is donated to CIAO3, which acts as mediator of the $[4Fe\text{-}4S]^{2+}$ cluster insertion into IRP1 and other cytosolic targets following two alternative pathways. In one pathway, CIAO3 interacts with CIAO1 and CIAO2A to deliver the $[4Fe\text{-}4S]^{2+}$ cluster to IRP1 thus generating aconitase. In the other pathway, CIAO3 interacts with CTC complex to deliver the $[4Fe\text{-}4S]^{2+}$ cluster to several cytosolic target apo proteins, including ABCE1, which requires the specific assistance of the YAE1-ORAOV1 complex. Red colour was used to highlight proteins and pathways that have been characterized through solution NMR. Structural models of human proteins, solved by X-ray crystallography or solution NMR, were reported. [2Fe-2S] clusters were represented as red and green (for Fe^{3+} and Fe^{2+}, respectively) and yellow (for S) spheres. PDB IDs are: CIAO1-3FM0, dimeric CIAO2A-3UX2, monomeric CIAO2A-2M5H and CIAO1-CIAO2B-MMS19 complex-6TC0.

However, the structure of YAE1-ORAOV1 is strongly required to validate this model.

4. Conclusions and outlook

The characterization of the mechanisms that drive Fe/S protein biogenesis is a crucial aspect both for the complete description of these pathways and for their impairment in rare diseases. The protein-protein interaction pathways herein described clearly show how, consistently with the premises summarized in the Introduction, solution NMR offers, at the same time, atomic scale resolution and unambiguous signatures of the oxidation and metalation state of the investigated systems. This makes solution NMR a unique technique to study cluster transfer, electron transfer and cluster assembly processes. The paramagnetism of Fe/S clusters represents an obstacle to the use of routine NMR experiments; however, as discussed in Section 2, the state of the art of our expertise combined with the recent improvements, in terms of sensitivity and versatility, of modern NMR instrumentation, allowed us to evade the loss of NMR information around the paramagnetic center and to convert pitfalls into challenges and limitations into advantages. Within this frame, we believe that solution NMR spectroscopy can play in the future a crucial role in addressing various molecular aspects of the Fe/S protein biogenesis as well as other emerging aspects, thanks to its unique ability, with respect to all the other structural methodologies, to simultaneously monitor protein-protein recognition, cluster transfer and electron transfer.

Another important argument that NMR studies have highlighted concerns the no requirement of input energy along cluster transfer pathways occurring after that the [2Fe-2S] cluster has been transferred from ISCU2 to GLRX5. Our NMR studies performed with GLRX5, ISCAs, IBA57, BOLAs, NFU1, LIAS showed indeed that the cluster transfer from the donor to the acceptor quantitatively occur without the need of energy ATP input. Therefore, the NMR data support a molecular model where properly tuned protein-protein interactions and cluster affinities in the proteins part of a cluster transfer pathway can create a thermodynamic cascade that brings the cluster to its final destination, i.e. the target protein/enzyme. The specific protein-protein recognition between the partner proteins along the pathway can also guarantee a rapid and selective cluster transfer process. It might be possible that, along a cluster transfer pathway, we can have incomplete cluster transfer reactions; however, the high affinity for cluster binding typical of the final target protein can pull this equilibrium toward the product and overcome a shallow thermodynamic gradient. This thermodynamic gradient-based model is what we have indeed showed to occur in the ISCA1-ISCA2-NFU1-dependent $[4Fe\text{-}4S]^{2+}$ cluster delivery pathway that specifically directs the cluster into the cluster-binding site of the final target LIAS protein [142]. This model is specular with what it has been already demonstrated by us and others in copper transfer pathways [214,215]. On the other hand, to definitively validate this model for iron-sulfur cluster transfer pathways, it would be vital in the future to develop probes able to quantitative compare the affinities of iron-sulfur-binding proteins on a reliable and unified scale, similarly to what it was done for copper chaperones/proteins [214].

CRediT authorship contribution statement

Leonardo Querci: Writing – review & editing, Writing – original draft, Visualization, Conceptualization. **Mario Piccioli:** Writing – review & editing, Writing – original draft, Visualization, Conceptualization. **Simone Ciofi-Baffoni:** Writing – review & editing, Writing –

original draft, Visualization, Supervision, Conceptualization. **Lucia Banci:** Writing – review & editing, Supervision, Conceptualization.

Declaration of competing interest

The authors declare that they have no known competing financial interests or personal relationships that could have appeared to influence the work reported in this paper.

Data availability

No data was used for the research described in the article.

Acknowledgements

The authors acknowledge the support by the Italian Ministry for University and Research (FOE funding) to the CERM/CIRMMP Italian Centre of Instruct-ERIC, a landmark ESFRI project. All authors acknowledge support from COST Action, FeSImmChemNet. This article is based upon work from COST Action FeSImmChemNet, CA21115, supported by COST (European Cooperation in Science and Technology). L.Q. is a PhD student under the Tuscany Health Ecosystem ECS_00000017 (CUP B83C22003920001), spoke 7, funded by the European Union-NextGeneration EU.

References

[1] W.D. Phillips, M. Poe, J.F. Weiher, C.C. McDonald, W. Lovenberg, Proton magnetic resonance, magnetic susceptibility and Mossbauer studies of *Clostridium pasteurianum* rubredoxin, Nature 227 (1970) 574–577.
[2] W.R. Dunham, G. Palmer, R.H. Sands, A.J. Bearden, On the structure of the iron-sulfur complex in the two-iron ferredoxins, Biochim. Biophys. Acta 253 (1971) 373–384.
[3] L. Banci, M. Piccioli, A. Scozzafava, Advancements in NMR investigation of paramagnetic molecules in solution, Coord. Chem. Rev. 120 (1992) 1–28.
[4] L. Banci, I. Bertini, S. Ciurli, S. Ferretti, C. Luchinat, M. Piccioli, The electronic structure of $(Fe_4S_4)^{3+}$ clusters in proteins. An investigation of the oxidized high-potential iron-sulfur protein II from *Ectothiorhodospira vacuolata*, Biochemistry 32 (1993) 9387–9397.
[5] L. Banci, I. Bertini, C. Luchinat, The ^{1}H NMR parameters of magnetically coupled dimers - the Fe_2S_2 proteins as an example, Struct. Bond. 72 (1990) 113–135.
[6] L.B. Dugad, G.N. La Mar, L. Banci, I. Bertini, Identification of localized redox states in plant-type two-iron ferredoxins using the nuclear overhauser effect, Biochemistry 29 (1990) 2263–2271.
[7] I. Bertini, F. Capozzi, S. Ciurli, C. Luchinat, L. Messori, M. Piccioli, Identification of the iron ions of HiPIP from *Chromatium vinosum* within the protein frame through 2D NMR experiments, J. Am. Chem. Soc. 114 (1992) 3332–3340.
[8] I. Bertini, F. Capozzi, C. Luchinat, M. Piccioli, A.J. Vila, The Fe_4S_4 centers in ferredoxins studied through proton and carbon hyperfine coupling. Sequence specific assignments of cysteines in ferredoxins from *Clostridium acidi urici* and *Clostridium pasteurianum*, J. Am. Chem. Soc. 116 (1994) 651–660.
[9] L. Banci, I. Bertini, F. Capozzi, P. Carloni, S. Ciurli, C. Luchinat, M. Piccioli, The iron-sulfur cluster in the oxidized high potential iron sulfur protein from *Ectothiorhodospira halophila*, J. Am. Chem. Soc. 115 (1993) 3431–3440.
[10] L. Banci, I. Bertini, P. Carloni, C. Luchinat, P.L. Orioli, Molecular dynamics simulations on HiPIP from *Chomatium vinosum* and comparison with NMR data, J. Am. Chem. Soc. 114 (1992) 10683–10689.
[11] L. Banci, F. Camponeschi, S. Ciofi-Baffoni, M. Piccioli, The NMR contribution to protein–protein networking in Fe–S protein maturation, J. Biol. Inorg. Chem. 23 (2018) 665–685.
[12] S. Todorovic, M. Teixeira, Resonance Raman spectroscopy of Fe–S proteins and their redox properties, J. Biol. Inorg. Chem. 23 (2018) 647–661.
[13] R. Garcia-Serres, M. Clemancey, J.M. Latour, G. Blondin, Contribution of Mossbauer spectroscopy to the investigation of Fe/S biogenesis, J. Biol. Inorg. Chem. 23 (2018) 635–644.
[14] W.R. Hagen, EPR spectroscopy of complex biological iron-sulfur systems, J. Biol. Inorg. Chem. 23 (2018) 623–634.
[15] S. Matteucci, F. Camponeschi, M. Clémancey, S. Ciofi-Baffoni, G. Blondin, L. Banci, In Cellulo Mössbauer and EPR studies bring new evidence to the long-standing debate on Iron-sulfur cluster binding in human Anamorsin, Angew. Chem. Int. Ed. Engl. 60 (2021) 14841–14845.
[16] H. Beinert, Iron-sulfur proteins: ancient structures, still full of surprises, J. Biol. Inorg. Chem. 5 (2000) 2–15.
[17] D. Brancaccio, A. Gallo, M. Mikolajczyk, K. Zovo, P. Palumaa, E. Novellino, M. Piccioli, S. Ciofi-Baffoni, L. Banci, Formation of [4Fe-4S] clusters in the mitochondrial iron-sulfur cluster assembly machinery, J. Am. Chem. Soc. 136 (2014) 16240–16250.
[18] L. Banci, F. Camponeschi, S. Ciofi-Baffoni, R. Muzzioli, Elucidating the molecular function of human BOLA2 in GRX3-dependent anamorsin maturation pathway, J. Am. Chem. Soc. 137 (2015) 16133–16134.
[19] M.A. Uzarska, V. Nasta, B.D. Weiler, F. Spantgar, S. Ciofi-Baffoni, M. Saviello, L. Gonnelli, U. Muhlenhoff, L. Banci, R. Lill, Mitochondrial Bol1 and Bol3 function as assembly factors for specific iron-sulfur proteins, Elife 5 (2016) e16673.
[20] S. Ciofi-Baffoni, V. Nasta, L. Banci, Protein networks in the maturation of human iron–sulfur proteins, Metallomics 10 (2018) 49–72.
[21] D. Grifagni, J.M. Silva, L. Querci, M. Lepoivre, C. Vallières, R.O. Louro, L. Banci, M. Piccioli, M.-P. Golinelli, F. Cantini, Biochemical and cellular characterization of the CISD3 protein: molecular bases of cluster release and destabilizing effects of nitric oxide, J. Biol. Chem. 300 (2024) 105745.
[22] F. Camponeschi, N.R. Prusty, S.A.E. Heider, S. Ciofi-Baffoni, L. Banci, GLRX3 acts as a [2Fe-2S] cluster chaperone in the cytosolic Iron-sulfur assembly machinery transferring [2Fe-2S] clusters to NUBP1, J. Am. Chem. Soc. 142 (2020) 10794–10805.
[23] S.A. Kassube, N.H. Thomä, Structural insights into Fe-S protein biogenesis by the CIA targeting complex, Nat. Struct. Mol. Biol. 27 (2020) 735–742.
[24] A. Ignatiou, K. Macé, A. Redzej, T.R.D. Costa, G. Waksman, E.V. Orlova, Structural analysis of protein complexes by Cryo-Electron microscopy, in: L. Journet, E. Cascales (Eds.), Bacterial Secretion Systems : Methods and Protocols, Springer, US, Place Published, 2024, pp. 431–470.
[25] C.W.J. Carter, J. Kraut, S.T. Freer, N.H. Xuong, R.A. Alden, R.G. Bartsch, Two-angstrom crystal structure of Chromatium vinosum high-potential iron protein, J. Biol. Chem. 249 (1974) 4212–4215.
[26] C.W.J. Carter, J. Kraut, S.T. Freer, R.A. Alden, Comparison of oxidation-reduction site geometries in oxidized and reduced Chromatium high potential iron protein and oxidized Peptococcus aerogenes ferredoxin, J. Biol. Chem. 249 (1974) 6339–6346.
[27] D.R. Breiter, T.E. Meyer, I. Rayment, H.M. Holden, The molecular structure of the high potential iron-sulfur protein isolated from *Ectothiorhodospira halophila* determined at 2.5 Å resolution, J. Biol. Chem. 266 (1991) 18660–18667.
[28] G. Backes, Y. Mino, T.M. Loehr, T.E. Meyer, M.A. Cusanovich, W.V. Sweeney, E. T. Adman, J. Sanders-Loehr, The environment of Fe_4S_4 cluster in ferredoxins and high- potential iron proteins. New information from X-ray crystallography and resonance Raman spectroscopy, J. Am. Chem. Soc. 113 (1991) 2055–2064.
[29] I. Rayment, G. Wesenberg, T.E. Meyer, M.A. Cusanovich, H.M. Holden, Three-dimensional structure of the high-potential iron-sulfur protein isolated from the purple phototrophic bacterium Rhodocyclus tenuis determined and refined at 1.5 a resolution, J. Mol. Biol. 228 (1992) 672–686.
[30] Y. Nicolet, R. Rohac, L. Martin, J.C. Fontecilla-Camps, X-ray snapshots of possible intermediates in the time course of synthesis and degradation of protein-bound Fe4S4 clusters, Proc. Natl. Acad. Sci. U. S. A. 110 (2013) 7188–7192.
[31] O. Karmi, H.B. Marjault, F. Bai, S. Roy, Y.S. Sohn, M. Darash Yahana, F. Morcos, K. Ioannidis, Y. Nahmias, P.A. Jennings, R. Mittler, J.N. Onuchic, R. Nechushtai, A VDAC1-mediated NEET protein chain transfers [2Fe-2S] clusters between the mitochondria and the cytosol and impacts mitochondrial dynamics, Proc. Natl. Acad. Sci. U. S. A. 119 (2022) e2121491119.
[32] K. Honarmand Ebrahimi, S. Ciofi-Baffoni, P.L. Hagedoorn, Y. Nicolet, N.E. Le Brun, W.R. Hagen, F.A. Armstrong, Iron-sulfur clusters as inhibitors and catalysts of viral replication, Nat. Chem. 14 (2022) 253–266.
[33] I. Bertini, C. Luchinat, G. Parigi, E. Ravera, NMR of Paramagnetic Molecules, Elsevier, Place Published, 2017.
[34] L. Querci, L. Fiorucci, E. Ravera, M. Piccioli, Paramagnetic Nuclear Magnetic Resonance: The Toolkit, Inorganics, 2024.
[35] G. Parigi, E. Ravera, C. Luchinat, Magnetic susceptibility and paramagnetism-based NMR, Prog Nucl Magn Reson, Spectrosc 114-115 (2019) 211–236.
[36] M. Piccioli, Paramagnetic NMR spectroscopy is a tool to address reactivity, structure, and protein-protein interactions of metalloproteins: the case of iron-sulfur proteins, Magnetochemistry 6 (2020) 46.
[37] J.C. Ott, E.A. Suturina, I. Kuprov, J. Nehrkorn, A. Schnegg, M. Enders, L.H. Gade, Observability of paramagnetic NMR signals at over 10 000 ppm chemical shifts, Angew. Chem. Int. Ed. Engl. 60 (2021) 22856–22864.
[38] I.B. Trindade, A. Coelho, F. Cantini, M. Piccioli, R.O. Louro, NMR of paramagnetic metalloproteins in solution: Ubi venire, quo vadis? J. Inorg. Biochem. 234 (2022) 111871.
[39] G. Parigi, E. Ravera, C. Luchinat, Paramagnetic effects in NMR for protein structures and ensembles: studies of metalloproteins, Curr. Op. Struct. Biol. 74 (2022) 102386.
[40] A. Swartjes, P.B. White, J.P.J. Bruekers, J.A.A.W. Elemans, R.J.M. Nolte, Paramagnetic relaxation enhancement NMR as a tool to probe guest binding and exchange in metallohosts, Nat. Commun. 13 (2022) 1846.
[41] N. Karschin, S. Becker, C. Griesinger, Interdomain dynamics via paramagnetic NMR on the highly flexible complex calmodulin/Munc13-1, J. Am. Chem. Soc. 144 (2022) 17041–17053.
[42] Q. Miao, C. Nitsche, H. Orton, M. Overhand, G. Otting, M. Ubbink, Paramagnetic chemical probes for studying biological macromolecules, Chem. Rev. 122 (2022) 9571–9642.
[43] H.W. Orton, G. Otting, Accurate Electron–Nucleus Distances from Paramagnetic Relaxation Enhancements, J. Am. Chem. Soc., 140 (2018) 7688–7697.
[44] C.A. Softley, M.J. Bostock, G.M. Popowicz, M. Sattler, Paramagnetic NMR in drug discovery, J. Biomol. NMR 74 (2020) 287–309.
[45] D. Parker, E.A. Suturina, I. Kuprov, N.F. Chilton, How the ligand field in lanthanide coordination complexes determines magnetic susceptibility

anisotropy, paramagnetic NMR shift, and relaxation behavior, Acc. Chem. Res. 53 (2020) 1520–1534.
[46] A. Bertarello, L. Benda, K. Sanders, A.J. Pell, M.J. Knight, V. Pelmenschikov, L. Gonnelli, I.C. Felli, M. Kaupp, L. Emsley, R. Pierattelli, G. Pintacuda, Picometer resolution structure of the coordination sphere in the metal-binding site in a metalloprotein by NMR, J. Am. Chem. Soc. 142 (2020) 16757–16765.
[47] L. Banci, I. Bertini, C. Luchinat, Nuclear and electron Relaxation. The Magnetic Nucleus-Unpaired electron Coupling in Solution, VCH, Place Published, 1991.
[48] F. Arnesano, L. Banci, M. Piccioli, NMR structures of paramagnetic metalloproteins, Q. Rev. Biophys. 38 (2005) 167–219.
[49] C. Luchinat, G. Parigi, E. Ravera, Paramagnetism in Experimental Biomolecular NMR, in: B. Balcom, I. Furó, M. Kainosho, M. Liu (Eds.), New Developments in NMR, Royal Society of Chemistry, Cambridge, 2018, p. 316.
[50] I.B. Trindade, M. Invernici, F. Cantini, R.O. Louro, M. Piccioli, (1)H, (13)C and (15)N assignment of the paramagnetic high potential iron-sulfur protein (HiPIP) PioC from Rhodopseudomonas palustris TIE-1, Biomol. NMR Assign. 14 (2020) 211–215.
[51] I. Bertini, C. Luchinat, G. Parigi, E. Ravera, NMR of Paramagnetic Molecules: Applications to Metallobiomolecules and Models, Elsevier, Place Published, 2016.
[52] I. Bertini, M.M. Couture, A. Donaire, L.D. Eltis, I.C. Felli, C. Luchinat, M. Piccioli, A. Rosato, The solution structure refinement of the paramagnetic reduced high-potential iron-sulfur protein I from Ectothiorhodospira halophila by using stable isotope labeling and nuclear relaxation, Eur. J. Biochem. 241 (1996) 440–452.
[53] L. Banci, Nuclear relaxation in paramagnetic metalloproteins, in: L.J. Berliner, J. Reuben (Eds.), Biological Magnetic Resonance, Plenum, Place Published, 1993, pp. 79–111.
[54] I. Bertini, A. Rosato, Solution structures of proteins containing paramagnetic metal ions, in: L. Banci, P. Comba (Eds.), Molecular Modeling and Dynamics of Bioinorganic Systems, Kluwer Academic Publishers, Place Published, 1997, pp. 1–19.
[55] L. Banci, C. Luchinat, Selective *versus* non-selective T_1 experiments to determine metal-nucleus distances in paramagnetic proteins, Inorg. Chim. Acta 373-379 (1998).
[56] F. Arnesano, L. Banci, I. Bertini, I.C. Felli, C. Luchinat, A.R. Thompsett, A strategy for the NMR characterization of type II copper(II) proteins: the case of the copper trafficking protein CopC from pseudomonas Syringae, J. Am. Chem. Soc. 125 (2003) 7200–7208.
[57] I.B. Trindade, M. Invernici, F. Cantini, R.O. Louro, M. Piccioli, PRE-driven protein NMR structures: an alternative approach in highly paramagnetic systems, FEBS J. 288 (2021) 3010–3023.
[58] L.Y. Lian, NMR studies of weak protein-protein interactions.
[59] L.Y. Lian, NMR studies of weak protein-protein interactions, Prog Nucl Magn Reson, Spectrosc 71 (2013) 59–72.
[60] K. Cai, J.L. Markley, NMR as a tool to investigate the processes of mitochondrial and cytosolic Iron-sulfur cluster biosynthesis, Molecules (Basel, Switzerland) 23 (2018) 2213.
[61] U. Kolczak, J. Salgado, G. Siegal, M. Saraste, G.W. Canters, Paramagnetic NMR studies of blue and purple copper proteins, Biospectroscopy 5 (1999) S19–S32.
[62] M. Piccioli, L. Poggi, Tailored HCCH–TOCSY experiment for resonance assignment in the proximity of a paramagnetic center, J. Magn. Reson. 155 (2002) 236–243.
[63] W. Bermel, I. Bertini, I.C. Felli, R. Kümmerle, R. Pierattelli, ^{13}C direct detection experiments on the paramagnetic oxidized monomeric copper, zinc superoxide dismutase, J. Am. Chem. Soc. 125 (2003) 16423–16429.
[64] W. Bermel, I. Bertini, L. Duma, L. Emsley, I.C. Felli, R. Pierattelli, P.R. Vasos, Complete assignment of heteronuclear protein resonances by protonless NMR spectroscopy, Angew. Chem. Int. Ed. 44 (2005) 3089–3092.
[65] W. Bermel, I. Bertini, I. Felli, M. Piccioli, R. Pierattelli, 13C-detected protonless NMR spectroscopy of proteins in solution, Prog. Nucl. Magn. Reson. Spectrosc. 48 (2006) 25–45.
[66] I.C. Felli, R. Pierattelli, (13)C direct detected NMR for challenging systems, Chem. Rev. 122 (2022) 9468–9496.
[67] I. Solomon, Relaxation processes in a system of two spins, Phys. Rev. 99 (1955) 559–565.
[68] F. Camponeschi, A. Gallo, M. Piccioli, L. Banci, The long-standing relationship between paramagnetic NMR and Iron-sulfur proteins: the mitoNEET example. An old method for new stories or the other way around? Magnetic Resonance Discussion 2 (2021) 203–211.
[69] F. Camponeschi, M. Piccioli, L. Banci, The intriguing mitoNEET: functional and spectroscopic properties of a unique [2Fe-2S] cluster coordination geometry, Molecules 27 (2022) 8218.
[70] D. Grifagni, J.M. Silva, F. Cantini, M. Piccioli, L. Banci, Relaxation-based NMR assignment: spotlights on ligand binding sites in human CISD3, J. Inorg. Biochem. 239 (2023) 112089.
[71] L. Querci, D. Grifagni, I.B. Trindade, J.M. Silva, R.O. Louro, F. Cantini, M. Piccioli, Paramagnetic NMR to study iron sulfur proteins: 13C detected experiments illuminate the vicinity of the metal center, J. Biomol. NMR 77 (2023) 247–259.
[72] L. Querci, I.B. Trindade, M. Invernici, J.M. Silva, F. Cantini, R.O. Louro, M. Piccioli, NMR of Paramagnetic Proteins: 13C Derived Paramagnetic Relaxation Enhancements Are an Additional Source of Structural Information in Solution, Magnetochemistry, 2023.
[73] M.T. Boniecki, S.A. Freibert, U. Muhlenhoff, R. Lill, M. Cygler, Structure and functional dynamics of the mitochondrial Fe/S cluster synthesis complex, Nat. Commun. 8 (2017) 1287.
[74] K. Cai, R.O. Frederick, H. Dashti, J.L. Markley, Architectural features of human mitochondrial cysteine Desulfurase complexes from crosslinking mass spectrometry and small-angle X-ray scattering, Structure 26 (2018) 1127–1136. e1124.
[75] N.G. Fox, X. Yu, X. Feng, H.J. Bailey, A. Martelli, J.F. Nabhan, C. Strain-Damerell, C. Bulawa, W.W. Yue, S. Han, Structure of the human frataxin-bound iron-sulfur cluster assembly complex provides insight into its activation mechanism, Nat. Commun. 10 (2019) 2210.
[76] K. Cai, R.O. Frederick, M. Tonelli, J.L. Markley, Interactions of iron-bound frataxin with ISCU and ferredoxin on the cysteine desulfurase complex leading to Fe-S cluster assembly, J. Inorg. Biochem. 183 (2018) 107–113.
[77] T. Yoon, J.A. Cowan, Iron-sulfur cluster biosynthesis. Characterization of frataxin as an iron donor for assembly of [2Fe-2S] clusters in ISU-type proteins, J. Am. Chem. Soc. 125 (2003) 6078–6084.
[78] J.D. Cook, K.Z. Bencze, A.D. Jankovic, A.K. Crater, C.N. Busch, P.B. Bradley, A. J. Stemmler, M.R. Spaller, T.L. Stemmler, Monomeric yeast Frataxin is an Iron-binding protein, Biochemistry 45 (2006) 7767–7777.
[79] K.C. Kondapalli, N.M. Kok, A. Dancis, T.L. Stemmler, Drosophila Frataxin: an Iron chaperone during cellular Fe−S cluster bioassembly, Biochemistry 47 (2008) 6917–6927.
[80] G. Layer, S. Ollagnier-de Choudens, Y. Sanakis, M. Fontecave, Iron-sulfur cluster biosynthesis: characterization of Escherichia coli CYaY as an iron donor for the assembly of [2Fe-2S] clusters in the scaffold IscU, J. Biol. Chem. 281 (2006) 16256–16263.
[81] A. Parent, X. Elduque, D. Cornu, L. Belot, J.P. Le Caer, A. Grandas, M.B. Toledano, B. D'Autréaux, Mammalian frataxin directly enhances sulfur transfer of NFS1 persulfide to both ISCU and free thiols, Nat. Commun. 6 (2015) 5686.
[82] J. Bridwell-Rabb, N.G. Fox, C.L. Tsai, A.M. Winn, D.P. Barondeau, Human frataxin activates Fe-S cluster biosynthesis by facilitating sulfur transfer chemistry, Biochemistry 53 (2014) 4904–4913.
[83] H. Yoon, S.A.B. Knight, A. Pandey, J. Pain, S. Turkarslan, D. Pain, A. Dancis, Turning Saccharomyces cerevisiae into a Frataxin-independent organism, PLoS Genet. 11 (2015) e1005135.
[84] H. Yoon, S.A. Knight, A. Pandey, J. Pain, Y. Zhang, D. Pain, A. Dancis, Frataxin-bypassing Isu1: characterization of the bypass activity in cells and mitochondria, Biochem. J. 459 (2014) 71–81.
[85] H. Yoon, R. Golla, E. Lesuisse, J. Pain, J.E. Donald, E.R. Lyver, D. Pain, A. Dancis, Mutation in the Fe-S scaffold protein Isu bypasses frataxin deletion, Biochem. J. 441 (2012) 473–480.
[86] K. Cai, R.O. Frederick, M. Tonelli, J.L. Markley, ISCU(M108I) and ISCU(D39V) differ from wild-type ISCU in their failure to form cysteine Desulfurase complexes containing both Frataxin and ferredoxin, Biochemistry 57 (2018) 1491–1500.
[87] Z. Dai, M. Tonelli, J.L. Markley, Metamorphic protein IscU changes conformation by cis-trans isomerizations of two peptidyl-prolyl peptide bonds, Biochemistry 51 (2012) 9595–9602.
[88] M.A. Uzarska, I. Grochowina, J. Soldek, M. Jelen, B. Schilke, J. Marszalek, E. A. Craig, R. Dutkiewicz, During FeS cluster biogenesis, ferredoxin and frataxin use overlapping binding sites on yeast cysteine desulfurase Nfs1, J. Biol. Chem. 298 (2022) 101570.
[89] R. Yan, P.V. Konarev, C. Iannuzzi, S. Adinolfi, B. Roche, G. Kelly, L. Simon, S. R. Martin, B. Py, F. Barras, D.I. Svergun, A. Pastore, Ferredoxin competes with bacterial frataxin in binding to the desulfurase IscS, J. Biol. Chem. 288 (2013) 24777–24787.
[90] S. Gervason, D. Larkem, A.B. Mansour, T. Botzanowski, C.S. Muller, L. Pecqueur, G. Le Pavec, A. Delaunay-Moisan, O. Brun, J. Agramunt, A. Grandas, M. Fontecave, V. Schunemann, S. Cianferani, C. Sizun, M.B. Toledano, B. D'Autreaux, Physiologically relevant reconstitution of iron-sulfur cluster biosynthesis uncovers persulfide-processing functions of ferredoxin-2 and frataxin, Nat. Commun. 10 (2019) 3566.
[91] V. Schulz, S. Basu, S.A. Freibert, H. Webert, L. Boss, U. Mühlenhoff, F. Pierrel, L. O. Essen, D.M. Warui, S.J. Booker, O. Stehling, R. Lill, Functional spectrum and specificity of mitochondrial ferredoxins FDX1 and FDX2, Nat. Chem. Biol. 19 (2023) 206–217.
[92] A.D. Sheftel, O. Stehling, A.J. Pierik, H.P. Elsasser, U. Muhlenhoff, H. Webert, A. Hobler, F. Hannemann, R. Bernhardt, R. Lill, Humans possess two mitochondrial ferredoxins, Fdx1 and Fdx2, with distinct roles in steroidogenesis, heme, and Fe/S cluster biosynthesis, Proc. Natl. Acad. Sci. U. S. A. 107 (2010) 11775–11780.
[93] K. Cai, M. Tonelli, R.O. Frederick, J.L. Markley, Human mitochondrial ferredoxin 1 (FDX1) and ferredoxin 2 (FDX2) both bind cysteine Desulfurase and donate electrons for Iron-sulfur cluster biosynthesis, Biochemistry 56 (2017) 487–499.
[94] L. Skjeldal, J.L. Markley, V.M. Coghlan, L.E. Vickery, ^{1}H-NMR spectra of vertebrate (2Fe-2S) ferredoxins. Hyperfine resonances suggest different electron delocalization patterns from plant ferredoxins, Biochemistry 30 (1991) 9078–9083.
[95] H. Webert, S.A. Freibert, A. Gallo, T. Heidenreich, U. Linne, S. Amlacher, E. Hurt, U. Muhlenhoff, L. Banci, R. Lill, Functional reconstitution of mitochondrial Fe/S cluster synthesis on Isu1 reveals the involvement of ferredoxin, Nat. Commun. 5 (2014) 5013.
[96] G. Kurisu, M. Kusunoki, E. Katoh, T. Yamazaki, K. Teshima, Y. Onda, Y. Kimata-Ariga, T. Hase, Structure of the electron transfer complex between ferredoxin and ferredoxin-NADP^{+} reductase, Nat. Struct. Biol. 8 (2001) 117–121.
[97] H. Ye, S.Y. Jeong, M.C. Ghosh, G. Kovtunovych, L. Silvestri, D. Ortillo, N. Uchida, J. Tisdale, C. Camaschella, T.A. Rouault, Glutaredoxin 5 deficiency causes sideroblastic anemia by specifically impairing heme biosynthesis and depleting cytosolic iron in human erythroblasts, J. Clin. Invest. 120 (2010) 1749–1761.

[98] R. Dutkiewicz, M. Nowak, Molecular chaperones involved in mitochondrial iron–sulfur protein biogenesis, J. Biol. Inorg. Chem. 23 (2018) 569–579.
[99] J. Marszalek, E.A. Craig, Interaction of client-the scaffold on which FeS clusters are build-with J-domain protein Hsc20 and its evolving Hsp70 partners, Front. Mol. Biosci. 9 (2022) 1034453.
[100] A.J. Andrew, R. Dutkiewicz, H. Knieszner, E.A. Craig, J. Marszalek, Characterization of the interaction between the J-protein Jac1p and the scaffold for Fe-S cluster biogenesis, Isu1p*, J. Biol. Chem. 281 (2006) 14580–14587.
[101] L.E. Vickery, J.R. Cupp-Vickery, Molecular chaperones HscA/Ssq1 and HscB/Jac1 and their roles in Iron-sulfur protein maturation, Crit. Rev. Biochem. Mol. Biol. 42 (2007) 95–111.
[102] K. Cai, R.O. Frederick, J.H. Kim, N.M. Reinen, M. Tonelli, J.L. Markley, Human mitochondrial chaperone (mtHSP70) and cysteine Desulfurase (NFS1) bind preferentially to the disordered conformation, whereas co-chaperone (HSC20) binds to the structured conformation of the Iron-sulfur cluster scaffold protein (ISCU), J. Biol. Chem. 288 (2013) 28755–28770.
[103] J. Marszalek, E.A. Craig, M. Pitek, R. Dutkiewicz, Chaperone function in Fe-S protein biogenesis: three possible scenarios, Biochimica et Biophysica Acta. Molecular Cell Research 1871 (2024) 119717.
[104] C. Johansson, A.K. Roos, S.J. Montano, R. Sengupta, P. Filippakopoulos, K. Guo, F. von Delft, A. Holmgren, U. Oppermann, K.L. Kavanagh, The crystal structure of human GLRX5: iron-sulfur cluster co-ordination, tetrameric assembly and monomer activity, Biochem. J. 433 (2011) 303–311.
[105] H. Li, C.E. Outten, Monothiol CGFS glutaredoxins and BolA-like proteins: [2Fe-2S] binding partners in iron homeostasis, Biochemistry 51 (2012) 4377–4389.
[106] L. Banci, D. Brancaccio, S. Ciofi-Baffoni, R. Del Conte, R. Gadepalli, M. Mikolajczyk, S. Neri, M. Piccioli, J. Winkelmann, [2Fe-2S] cluster transfer in iron-sulfur protein biogenesis, Proc. Natl. Acad. Sci. U. S. A. 111 (2014) 6203–6208.
[107] S. Ciofi-Baffoni, A. Gallo, R. Muzzioli, M. Piccioli, The IR-(1)(5)N-HSQC-AP experiment: a new tool for NMR spectroscopy of paramagnetic molecules, J. Biomol. NMR 58 (2014) 123–128.
[108] E.A. Talib, C.E. Outten, Iron-sulfur cluster biogenesis, trafficking, and signaling: roles for CGFS glutaredoxins and BolA proteins, Biochimica et Biophysica acta. Molecular Cell Research 1868 (2020) 118847.
[109] J.M. Cameron, A. Janer, V. Levandovskiy, N. MacKay, T.A. Rouault, W.H. Tong, I. Ogilvie, E.A. Shoubridge, B.H. Robinson, Mutations in iron-sulfur cluster scaffold genes NFU1 and BOLA3 cause a fatal deficiency of multiple respiratory chain and 2-oxoacid dehydrogenase enzymes, Am. J. Hum. Genet. 89 (2011) 486–495.
[110] A. Navarro-Sastre, F. Tort, O. Stehling, M.A. Uzarska, J.A. Arranz, T.M. Del, M. T. Labayru, J. Landa, A. Font, J. Garcia-Villoria, B. Merinero, M. Ugarte, L. G. Gutierrez-Solana, J. Campistol, A. Garcia-Cazorla, J. Vaquerizo, E. Riudor, P. Briones, O. Elpeleg, A. Ribes, R. Lill, A fatal mitochondrial disease is associated with defective NFU1 function in the maturation of a subset of mitochondrial Fe-S proteins, Am. J. Hum. Genet. 89 (2011) 656–667.
[111] P. Willems, B.F. Wanschers, J. Esseling, R. Szklarczyk, U. Kudla, I. Duarte, M. Forkink, M. Nooteboom, H. Swarts, J. Gloerich, L. Nijtmans, W. Koopman, M. A. Huynen, BOLA1 is an aerobic protein that prevents mitochondrial morphology changes induced by glutathione depletion, Antioxid. Redox, Signal 18 (2013) 129–138.
[112] V. Nasta, A. Giachetti, S. Ciofi-Baffoni, L. Banci, Structural insights into the molecular function of human (2Fe-2S) BOLA1-GRX5 and (2Fe-2S) BOLA3-GRX5 complexes, Biochim. Biophys. Acta 2017 (1861) 2119–2131.
[113] H. Zhong, A. Janer, O. Khalimonchuk, H. Antonicka, Eric A. Shoubridge, A. Barrientos, BOLA3 and NFU1 link mitoribosome iron–sulfur cluster assembly to multiple mitochondrial dysfunctions syndrome, Nucleic Acids Res. 51 (2023) 11797–11812.
[114] S. Sen, B. Rao, C. Wachnowsky, J.A. Cowan, Cluster exchange reactivity of [2Fe-2S] cluster-bridged complexes of BOLA3 with monothiol glutaredoxins, Metallomics 10 (2018) 1282–1290.
[115] V. Nasta, D. Suraci, S. Gourdoupis, S. Ciofi-Baffoni, L. Banci, A pathway for assembling $[4Fe\text{-}4S]^{2+}$ clusters in mitochondrial iron-sulfur protein biogenesis, FEBS J. 287 (2020) 2312–2327.
[116] S. Sen, A.L. Hendricks, J.A. Cowan, Cluster exchange reactivity of [2Fe-2S]-bridged heterodimeric BOLA1-GLRX5, FEBS J. 288 (2021) 920–929.
[117] A.D. Sheftel, C. Wilbrecht, O. Stehling, B. Niggemeyer, H.P. Elsasser, U. Muhlenhoff, R. Lill, The human mitochondrial ISCA1, ISCA2, and IBA57 proteins are required for [4Fe-4S] protein maturation, Mol. Biol. Cell 23 (2012) 1157–1166.
[118] L.K. Beilschmidt, S. Ollagnier de Choudens, M. Fournier, I. Sanakis, M. A. Hograindleur, M. Clemancey, G. Blondin, S. Schmucker, A. Eisenmann, A. Weiss, P. Koebel, N. Messaddeq, H. Puccio, A. Martelli, ISCA1 is essential for mitochondrial Fe4S4 biogenesis in vivo, Nat. Commun. 8 (2017) 15124.
[119] E. Lebigot, M. Schiff, M.P. Golinelli-Cohen, A review of multiple mitochondrial dysfunction syndromes, syndromes associated with defective Fe-S protein maturation, Biomedicines 9 (2021) 989.
[120] F. Camponeschi, S. Ciofi-Baffoni, V. Calderone, L. Banci, Molecular basis of rare diseases associated to the maturation of mitochondrial [4Fe-4S]-containing proteins, Biomolecules 12 (2022) 1009.
[121] K.D. Kim, W.H. Chung, H.J. Kim, K.C. Lee, J.H. Roe, Monothiol glutaredoxin Grx5 interacts with Fe-S scaffold proteins Isa1 and Isa2 and supports Fe-S assembly and DNA integrity in mitochondria of fission yeast, Biochem. Biophys. Res. Commun. 392 (2010) 467–472.
[122] D.T. Mapolelo, B. Zhang, S. Randeniya, A.N. Albetel, H. Li, J. Couturier, C. E. Outten, N. Rouhier, M.K. Johnson, Monothiol glutaredoxins and A-type proteins: partners in Fe-S cluster trafficking, Dalton Trans. 42 (2013) 3107–3115.
[123] D. Brancaccio, A. Gallo, M. Piccioli, E. Novellino, S. Ciofi-Baffoni, L. Banci, [4Fe-4S] cluster assembly in mitochondria and its impairment by copper, J. Am. Chem. Soc. 139 (2017) 719–730.
[124] B.D. Weiler, M.C. Brück, I. Kothe, E. Bill, R. Lill, U. Mühlenhoff, Mitochondrial [4Fe-4S] protein assembly involves reductive [2Fe-2S] cluster fusion on ISCA1-ISCA2 by electron flow from ferredoxin FDX2, Proc. Natl. Acad. Sci. U. S. A. 117 (2020) 20555–20565.
[125] P.R. Joshi, S. Sadre, X.A. Guo, J.G. McCoy, V.K. Mootha, Lipoylation is dependent on the ferredoxin FDX1 and dispensable under hypoxia in human cells, J. Biol. Chem. 299 (2023) 105075.
[126] M. Zulkifli, A.U. Okonkwo, V.M. Gohil, FDX1 is required for the biogenesis of mitochondrial cytochrome c oxidase in mammalian cells, J. Mol. Biol. 435 (2023) 168317.
[127] S. Gourdoupis, V. Nasta, V. Calderone, S. Ciofi-Baffoni, L. Banci, IBA57 recruits ISCA2 to form a [2Fe-2S] cluster-mediated complex, J. Am. Chem. Soc. 140 (2018) 14401–14412.
[128] U. Mühlenhoff, B.D. Weiler, F. Nadler, R. Millar, I. Kothe, S.A. Freibert, F. Altegoer, G. Bange, R. Lill, The iron-sulfur cluster assembly (ISC) protein Iba57 executes a tetrahydrofolate-independent function in mitochondrial [4Fe-4S] protein maturation, J. Biol. Chem. 298 (2022) 102465.
[129] V. Nasta, S. Da Vela, S. Gourdoupis, S. Ciofi-Baffoni, D.I. Svergun, L. Banci, Structural properties of [2Fe-2S] ISCA2-IBA57: a complex of the mitochondrial iron-sulfur cluster assembly machinery, Sci. Rep. 9 (2019) 18986.
[130] E.L. McCarthy, S.J. Booker, Destruction and reformation of an iron-sulfur cluster during catalysis by lipoyl synthase, Science 358 (2017) 373–377.
[131] K. Cai, G. Liu, R.O. Frederick, R. Xiao, G.T. Montelione, J.L. Markley, Structural/functional properties of human NFU1, an intermediate [4Fe-4S] carrier in human mitochondrial Iron-sulfur cluster biogenesis, Structure 24 (2016) 2080–2091.
[132] D. Suraci, G. Saudino, V. Nasta, S. Ciofi-Baffoni, L. Banci, ISCA1 orchestrates ISCA2 and NFU1 in the maturation of human mitochondrial [4Fe-4S] proteins, J. Mol. Biol. 433 (2021) 166924.
[133] S. Da Vela, G. Saudino, F. Lucarelli, L. Banci, D.I. Svergun, S. Ciofi-Baffoni, Structural plasticity of NFU1 upon interaction with binding partners: insights into the mitochondrial [4Fe-4S] cluster pathway, J. Mol. Biol. 435 (2023) 168154.
[134] M. Fontecave, S. Ollagnier-de-Choudens, E. Mulliez, Biological radical sulfur insertion reactions, Chem. Rev. 103 (2003) 2149–2166.
[135] N.D. Lanz, S.J. Booker, Auxiliary iron-sulfur cofactors in radical SAM enzymes, Biochim. Biophys. Acta 2015 (1853) 1316–1334.
[136] F. Camponeschi, R. Muzzioli, S. Ciofi-Baffoni, M. Piccioli, L. Banci, Paramagnetic (1)H NMR spectroscopy to investigate the catalytic mechanism of radical S-Adenosylmethionine enzymes, J. Mol. Biol. 431 (2019) 4514–4522.
[137] A.L. Hendricks, C. Wachnowsky, B. Fries, I. Fidai, J.A. Cowan, Characterization and reconstitution of human Lipoyl synthase (LIAS) supports ISCA2 and ISCU as primary cluster donors and an ordered mechanism of cluster assembly, Int. J. Mol. Sci. 22 (2021) 1598.
[138] N.D. Lanz, J.M. Rectenwald, B. Wang, E.S. Kakar, T.N. Laremore, S.J. Booker, A. Silakov, Characterization of a radical intermediate in Lipoyl cofactor biosynthesis, J. Am. Chem. Soc. 137 (2015) 13216–13219.
[139] M.I. McLaughlin, N.D. Lanz, P.J. Goldman, K.H. Lee, S.J. Booker, C.L. Drennan, Crystallographic snapshots of sulfur insertion by lipoyl synthase, Proc. Natl. Acad. Sci. U. S. A. 113 (2016) 9446–9450.
[140] A. Jain, A. Singh, N. Maio, T.A. Rouault, Assembly of the [4Fe-4S] cluster of NFU1 requires the coordinated donation of two [2Fe-2S] clusters from the scaffold proteins, ISCU2 and ISCA1, Hum. Mol. Genet. 29 (2020) 3165–3182.
[141] E. Lebigot, P. Gaignard, I. Dorboz, A. Slama, M. Rio, P. de Lonlay, B. Heron, F. Sabourdy, O. Boespflug-Tanguy, A. Cardoso, F. Habarou, C. Ottolenghi, P. Therond, C. Bouton, M.P. Golinelli-Cohen, A. Boutron, Impact of mutations within the [Fe-S] cluster or the lipoic acid biosynthesis pathways on mitochondrial protein expression profiles in fibroblasts from patients, Mol. Genet. Metab. 122 (2017) 85–94.
[142] G. Saudino, S. Ciofi-Baffoni, L. Banci, Protein-interaction affinity gradient drives [4Fe-4S] cluster insertion in human Lipoyl synthase, J. Am. Chem. Soc. 144 (2022) 5713–5717.
[143] D.M. Warui, D. Sil, K.H. Lee, S.S. Neti, O.A. Esakova, H.L. Knox, C. Krebs, S. J. Booker, In vitro demonstration of human Lipoyl synthase catalytic activity in the presence of NFU1, ACS Bio & Med Chem Au 2 (2022) 456–468.
[144] E.L. McCarthy, A.N. Rankin, Z.R. Dill, S.J. Booker, The A-type domain in Escherichia coli NfuA is required for regenerating the auxiliary [4Fe-4S] cluster in Escherichia coli lipoyl synthase, J. Biol. Chem. 294 (2019) 1609–1617.
[145] B. Py, C. Gerez, S. Angelini, R. Planel, D. Vinella, L. Loiseau, E. Talla, C. Brochier-Armanet, S.R. Garcia, J.M. Latour, C.S. Ollagnier-de, M. Fontecave, F. Barras, Molecular organization, biochemical function, cellular role and evolution of NfuA, an atypical Fe-S carrier, Mol. Microbiol. 86 (2012) 155–171.
[146] K. Cai, R.O. Frederick, J.L. Markley, ISCU interacts with NFU1, and ISCU[4Fe-4S] transfers its Fe-S cluster to NFU1 leading to the production of holo-NFU1, J. Struct. Biol. 210 (2020) 107491.
[147] F. Colin, A. Martelli, M. Clemancey, J.M. Latour, S. Gambarelli, L. Zeppieri, C. Birck, A. Page, H. Puccio, C.S. de Ollagnier, Mammalian frataxin controls sulfur production and iron entry during de novo Fe4S4 cluster assembly, J. Am. Chem. Soc. 135 (2013) 733–740.
[148] N.G. Fox, M. Chakrabarti, S.P. McCormick, P.A. Lindahl, D.P. Barondeau, The human Iron-sulfur assembly complex catalyzes the synthesis of [2Fe-2S] clusters

on ISCU2 that can be transferred to acceptor molecules, Biochemistry 54 (2015) 3871–3879.
[149] A. Melber, U. Na, A. Vashisht, B.D. Weiler, R. Lill, J.A. Wohlschlegel, D.R. Winge, Role of Nfu1 and Bol3 in iron-sulfur cluster transfer to mitochondrial clients, Elife 5 (2016) e15991.
[150] G. Kispal, P. Csere, C. Prohl, R. Lill, The mitochondrial proteins Atm1p and Nfs1p are essential for biogenesis of cytosolic Fe/S proteins, EMBO J. 18 (1999) 3981–3989.
[151] J.J. Braymer, R. Lill, Iron-sulfur cluster biogenesis and trafficking in mitochondria, J. Biol. Chem. 292 (2017) 12754–12763.
[152] K.S. Kim, N. Maio, A. Singh, T.A. Rouault, Cytosolic HSC20 integrates de novo iron-sulfur cluster biogenesis with the CIAO1-mediated transfer to recipients, Hum. Mol. Genet. 27 (2018) 837–852.
[153] T.A. Rouault, The indispensable role of mammalian iron sulfur proteins in function and regulation of multiple diverse metabolic pathways, Biometals 32 (2019) 343–353.
[154] S. Ciofi-Baffoni, C. Andreini, The intriguing role of Iron-sulfur clusters in the CIAPIN1 protein family, Inorganics 10 (2022) 52.
[155] D.J. Netz, M. Stumpfig, C. Dore, U. Muhlenhoff, A.J. Pierik, R. Lill, Tah18 transfers electrons to Dre2 in cytosolic iron-sulfur protein biogenesis, Nat. Chem. Biol. 6 (2010) 758–765.
[156] L. Banci, I. Bertini, S. Ciofi-Baffoni, F. Boscaro, A. Chatzi, M. Mikolajczyk, K. Tokatlidis, J. Winkelmann, Anamorsin is a 2Fe2S cluster-containing substrate of the Mia40-dependent mitochondrial protein trapping machinery, Chem. Biol. 18 (2011) 794–804.
[157] L. Banci, I. Bertini, V. Calderone, S. Ciofi-Baffoni, A. Giachetti, D. Jaiswal, M. Mikolajczyk, M. Piccioli, J. Winkelmann, Molecular view of an electron transfer process essential for iron-sulfur protein biogenesis, Proc. Natl. Acad. Sci. U. S. A. 110 (2013) 7136–7141.
[158] C. Andreini, S. Ciofi-Baffoni, Basic Iron-Sulfur Centers, Metal ions in life sciences, 2020.
[159] L. Banci, S. Ciofi-Baffoni, M. Mikolajczyk, J. Winkelmann, E. Bill, M.E. Pandelia, Human anamorsin binds [2Fe-2S] clusters with unique electronic properties, J. Biol. Inorg. Chem. 18 (2013) 883–893.
[160] N. Soler, C.T. Craescu, J. Gallay, Y.M. Frapart, D. Mansuy, B. Raynal, G. Baldacci, A. Pastore, M.E. Huang, L. Vernis, A S-adenosylmethionine methyltransferase-like domain within the essential, Fe-S-containing yeast protein Dre2, FEBS J. 279 (2012) 2108–2119.
[161] Y. Zhang, C. Yang, A. Dancis, E. Nakamaru-Ogiso, EPR studies of wild type and mutant Dre2 identify essential [2Fe–2S] and [4Fe–4S] clusters and their cysteine ligands, J. Biochem., 161 (2017) 67–78.
[162] D.J. Netz, H.M. Genau, B.D. Weiler, E. Bill, A.J. Pierik, R. Lill, The conserved protein Dre2 uses essential [2Fe-2S] and [4Fe-4S] clusters for its function in cytosolic iron-sulfur protein assembly, Biochem. J. 473 (2016) 2073–2085.
[163] Y. Zhang, E.R. Lyver, E. Nakamaru-Ogiso, H. Yoon, B. Amutha, D.W. Lee, E. Bi, T. Ohnishi, F. Daldal, D. Pain, A. Dancis, Dre2, a conserved eukaryotic Fe/S cluster protein, functions in cytosolic Fe/S protein biogenesis, Mol. Cell. Biol. 28 (2008) 5569–5582.
[164] O. Stehling, D.J. Netz, B. Niggemeyer, R. Rosser, R.S. Eisenstein, H. Puccio, A. J. Pierik, R. Lill, Human Nbp35 is essential for both cytosolic iron-sulfur protein assembly and iron homeostasis, Mol. Cell. Biol. 28 (2008) 5517–5528.
[165] D.J. Netz, A.J. Pierik, M. Stumpfig, E. Bill, A.K. Sharma, L.J. Pallesen, W. E. Walden, R. Lill, A bridging [4Fe-4S] cluster and nucleotide binding are essential for function of the Cfd1-Nbp35 complex as a scaffold in iron-sulfur protein maturation, J. Biol. Chem. 287 (2012) 12365–12378.
[166] B. Bargagna, S. Matteucci, S. Ciofi-Baffoni, F. Camponeschi, L. Banci, Unraveling the mechanism of [4Fe-4S] cluster assembly on the N-terminal cluster binding site of NUBP1, Protein Sci. 32 (2023) e4625.
[167] J.J. Braymer, S.A. Freibert, M. Rakwalska-Bange, R. Lill, Mechanistic concepts of iron-sulfur protein biogenesis in biology, Biochimica et Biophysica Acta. Molecular Cell Research 1868 (2021) 118863.
[168] H. Li, D.T. Mapolelo, S. Randeniya, M.K. Johnson, C.E. Outten, Human glutaredoxin 3 forms [2Fe-2S]-bridged complexes with human BolA2, Biochemistry 51 (2012) 1687–1696.
[169] P. Haunhorst, C. Berndt, S. Eitner, J.R. Godoy, C.H. Lillig, Characterization of the human monothiol glutaredoxin 3 (PICOT) as iron-sulfur protein, Biochem. Biophys. Res. Commun. 394 (2010) 372–376.
[170] L. Banci, S. Ciofi-Baffoni, K. Gajda, R. Muzzioli, R. Peruzzini, J. Winkelmann, N-terminal domains mediate [2Fe-2S] cluster transfer from glutaredoxin-3 to anamorsin, Nat. Chem. Biol. 11 (2015) 772–778.
[171] S. Sen, J.A. Cowan, Role of protein-glutathione contacts in defining glutaredoxin-3 [2Fe–2S] cluster chirality, ligand exchange and transfer chemistry, J. Biol. Inorg. Chem. 22 (2017) 1075–1087.
[172] D.J. Netz, A.J. Pierik, M. Stumpfig, U. Muhlenhoff, R. Lill, The Cfd1-Nbp35 complex acts as a scaffold for iron-sulfur protein assembly in the yeast cytosol, Nat. Chem. Biol. 3 (2007) 278–286.
[173] S. Tamir, M.L. Paddock, M. Darash-Yahana-Baram, S.H. Holt, Y.S. Sohn, L. Agranat, D. Michaeli, J.T. Stofleth, C.H. Lipper, F. Morcos, I.Z. Cabantchik, J. N. Onuchic, P.A. Jennings, R. Mittler, R. Nechushtai, Structure-function analysis of NEET proteins uncovers their role as key regulators of iron and ROS homeostasis in health and disease, Biochim. Biophys. Acta 2015 (1853) 1294–1315.
[174] F. Camponeschi, S. Ciofi-Baffoni, L. Banci, Anamorsin/Ndor1 complex reduces [2Fe-2S]-MitoNEET via a transient protein-protein interaction, J. Am. Chem. Soc. 139 (2017) 9479–9482.
[175] I. Ferecatu, S. Goncalves, M.P. Golinelli-Cohen, M. Clemancey, A. Martelli, S. Riquier, E. Guittet, J.M. Latour, H. Puccio, J.C. Drapier, E. Lescop, C. Bouton, The diabetes drug target MitoNEET governs a novel trafficking pathway to rebuild an Fe-S cluster into cytosolic aconitase/iron regulatory protein 1, J. Biol. Chem. 289 (2014) 28070–28086.
[176] O. Karmi, H.B. Marjault, L. Pesce, P. Carloni, J.N. Onuchic, P.A. Jennings, R. Mittler, R. Nechushtai, The unique fold and lability of the [2Fe-2S] clusters of NEET proteins mediate their key functions in health and disease, J. Biol. Inorg. Chem. 23 (2018) 599–612.
[177] C.H. Lipper, M.L. Paddock, J.N. Onuchic, R. Mittler, R. Nechushtai, P.A. Jennings, Cancer-related NEET proteins transfer 2Fe-2S clusters to Anamorsin, a protein required for cytosolic Iron-sulfur cluster biogenesis, PloS One 10 (2015) e0139699.
[178] J.A. Zuris, Y. Harir, A.R. Conlan, M. Shvartsman, D. Michaeli, S. Tamir, M. L. Paddock, J.N. Onuchic, R. Mittler, Z.I. Cabantchik, P.A. Jennings, R. Nechushtai, Facile transfer of [2Fe-2S] clusters from the diabetes drug target mitoNEET to an apo-acceptor protein, Proc. Natl. Acad. Sci. U. S. A. 108 (2011) 13047–13052.
[179] M.P. Golinelli-Cohen, E. Lescop, C. Mons, S. Goncalves, M. Clemancey, J. Santolini, E. Guittet, G. Blondin, J.M. Latour, C. Bouton, Redox control of the human Iron-sulfur repair protein MitoNEET activity via its Iron-sulfur cluster, J. Biol. Chem. 291 (2016) 7583–7593.
[180] K. Zuo, H.-B. Marjault, K.L. Bren, G. Rossetti, R. Nechushtai, P. Carloni, The two redox states of the human NEET proteins' [2Fe–2S] clusters, J. Biol. Inorg. Chem. 26 (2021) 763–774.
[181] L. Vernis, C. Facca, E. Delagoutte, N. Soler, R. Chanet, B. Guiard, G. Faye, G. Baldacci, A newly identified essential complex, Dre2-Tah18, controls mitochondria integrity and cell death after oxidative stress in yeast, PloS One 4 (2009) e4376.
[182] A.G. Frey, D.J. Palenchar, J.D. Wildemann, C.C. Philpott, A Glutaredoxin-BolA complex serves as an Iron-sulfur cluster chaperone for the cytosolic cluster assembly machinery, J. Biol. Chem. 291 (2016) 22344–22356.
[183] Y. Saito, H. Shibayama, H. Tanaka, A. Tanimura, I. Matsumura, Y. Kanakura, PICOT is a molecule which binds to anamorsin, Biochem. Biophys. Res. Commun. 408 (2011) 329–333.
[184] K. Luck, D.K. Kim, L. Lambourne, K. Spirohn, B.E. Begg, W. Bian, R. Brignall, T. Cafarelli, F.J. Campos-Laborie, B. Charloteaux, D. Choi, A.G. Coté, M. Daley, S. Deimling, A. Desbuleux, A. Dricot, M. Gebbia, M.F. Hardy, N. Kishore, J.J. Knapp, I.A. Kovács, I. Lemmens, M.W. Mee, J.C. Mellor, C. Pollis, C. Pons, A.D. Richardson, S. Schlabach, B. Teeking, A. Yadav, M. Babor, D. Balcha, O. Basha, C. Bowman-Colin, S.F. Chin, S.G. Choi, C. Colabella, G. Coppin, C. D'Amata, D. De Ridder, S. De Rouck, M. Duran-Frigola, H. Ennajdaoui, F. Goebels, L. Goehring, A. Gopal, G. Haddad, *E. hatchi*, M. Helmy, Y. Jacob, Y. Kassa, S. Landini, R. Li, N. van Lieshout, A. MacWilliams, D. Markey, J.N. Paulson, S. Rangarajan, J. Rasla, A. Rayhan, T. Rolland, A. San-Miguel, Y. Shen, D. Sheykhkarimli, G.M. Sheynkman, E. Simonovsky, M. Taşan, A. Tejeda, V. Tropepe, J.C. Twizere, Y. Wang, R.J. Weatheritt, J. Weile, Y. Xia, X. Yang, E. Yeger-Lotem, Q. Zhong, P. Aloy, G.D. Bader, J. De Las Rivas, S. Gaudet, T. Hao, J. Rak, J. Tavernier, D.E. Hill, M. Vidal, F.P. Roth, M.A. Calderwood, A reference map of the human binary protein interactome, Nature, 580 (2020) 402–408.
[185] Y.B. Zhou, J.B. Cao, B.B. Wan, X.R. Wang, G.H. Ding, H. Zhu, H.M. Yang, K. S. Wang, X. Zhang, Z.G. Han, hBolA, novel non-classical secreted proteins, belonging to different BolA family with functional divergence, Mol. Cell. Biochem. 317 (2008) 61–68.
[186] X. Nuttle, G. Giannuzzi, M.H. Duyzend, J.G. Schraiber, I. Narvaiza, F. Camponeschi, S. Ciofi-Baffoni, P.H. Sudmant, O. Penn, G. Chiatante, M. Malig, J. Huddleston, C. Benner, H.A.F. Stessman, M.C.N. Marchetto, L. Denman, L. Harshman, C. Baker, A. Raja, K. Penewit, W.J. Tang, M. Ventura, F. Antonacci, J.M. Akey, C.T. Amemiya, L. Banci, F.H. Gage, A. Reymond, E.E. Eichler, Emergence of a *Homo sapiens*-specific gene family and the evolution of autism risk at chromosome 16p11.2, Nature 536 (2016) 205–209.
[187] G. Giannuzzi, P.J. Schmidt, E. Porcu, G. Willemin, K.M. Munson, X. Nuttle, R. Earl, J. Chrast, K. Hoekzema, D. Risso, K. Männik, P. De Nittis, E.D. Baratz, Y. Herault, X. Gao, C.C. Philpott, R.A. Bernier, Z. Kutalik, M.D. Fleming, E. E. Eichler, A. Reymond, The human-specific BOLA2 duplication modifies Iron homeostasis and Anemia predisposition in chromosome 16p11.2 autism individuals, Am. J. Hum. Genet. 105 (2019) 947–958.
[188] R. Lill, V. Srinivasan, U. Muhlenhoff, The role of mitochondria in cytosolic-nuclear iron-sulfur protein biogenesis and in cellular iron regulation, Curr. Opin. Microbiol. 22 (2014) 111–119.
[189] A.K. Pandey, J. Pain, B. J., A. Dancis, D. Pain, Essential mitochondrial role in iron-sulfur cluster assembly of the cytoplasmic isopropylmalate isomerase Leu1 in Saccharomyces cerevisiae, Mitochondrion 69 (2023) 104–115.
[190] N. Maio, T.A. Rouault, Mammalian iron sulfur cluster biogenesis and human diseases, IUBMB Life 74 (2022) 705–714.
[191] N. Maio, T.A. Rouault, Mammalian iron sulfur cluster biogenesis: from assembly to delivery to recipient proteins with a focus on novel targets of the chaperone and co-chaperone proteins, IUBMB Life 74 (2022) 684–704.
[192] P. Li, A.L. Hendricks, Y. Wang, R.L.E. Villones, K. Lindkvist-Petersson, G. Meloni, J.A. Cowan, K. Wang, P. Gourdon, Structures of Atm1 provide insight into [2Fe-2S] cluster export from mitochondria, Nat. Commun. 13 (2022) 4339.
[193] S.J. Patel, A.G. Frey, D.J. Palenchar, S. Achar, K.Z. Bullough, A. Vashisht, J. A. Wohlschlegel, C.C. Philpott, A PCBP1-BolA2 chaperone complex delivers iron for cytosolic [2Fe-2S] cluster assembly, Nat. Chem. Biol. 15 (2019) 872–881.
[194] S.J. Patel, O. Protchenko, M. Shakoury-Elizeh, E. Baratz, S. Jadhav, C.C. Philpott, The iron chaperone and nucleic acid-binding activities of poly(rC)-binding

protein 1 are separable and independently essential, Proc. Natl. Acad. Sci. U. S. A. 118 (2021) e2104666118.
[195] V. Peleh, J. Riemer, A. Dancis, J.M. Herrmann, Protein oxidation in the intermembrane space of mitochondria is substrate-specific rather than general, Microb. Cell 1 (2014) 81–93.
[196] V.D. Paul, R. Lill, Biogenesis of cytosolic and nuclear iron-sulfur proteins and their role in genome stability, Biochim. Biophys. Acta 2015 (1853) 1528–1539.
[197] M. Seki, Y. Takeda, K. Iwai, K. Tanaka, IOP1 protein is an external component of the human cytosolic iron-sulfur cluster assembly (CIA) machinery and functions in the MMS19 protein-dependent CIA pathway, J. Biol. Chem. 288 (2013) 16680–16689.
[198] O. Stehling, A.A. Vashisht, J. Mascarenhas, Z.O. Jonsson, T. Sharma, D.J. Netz, A. J. Pierik, J.A. Wohlschlegel, R. Lill, MMS19 assembles iron-sulfur proteins required for DNA metabolism and genomic integrity, Science 337 (2012) 195–199.
[199] J. Balk, D.J. Aguilar Netz, K. Tepper, A.J. Pierik, R. Lill, The essential WD40 protein Cia1 is involved in a late step of cytosolic and nuclear iron-sulfur protein assembly, Mol. Cell. Biol. 25 (2005) 10833–10841.
[200] O. Stehling, J. Mascarenhas, A.A. Vashisht, A.D. Sheftel, B. Niggemeyer, R. Rosser, A.J. Pierik, J.A. Wohlschlegel, R. Lill, Human CIA2A-FAM96A and CIA2B-FAM96B integrate iron homeostasis and maturation of different subsets of cytosolic-nuclear iron-sulfur proteins, Cell Metab. 18 (2013) 187–198.
[201] K. Gari, A.M. Leon Ortiz, V. Borel, H. Flynn, J.M. Skehel, S.J. Boulton, MMS19 links cytoplasmic iron-sulfur cluster assembly to DNA metabolism, Science 337 (2012) 243–245.
[202] X. Fan, W.D. Barshop, A.A. Vashisht, V. Pandey, S. Leal, S. Rayatpisheh, Y. Jami-Alahmadi, J. Sha, J.A. Wohlschlegel, Iron-regulated assembly of the cytosolic iron-sulfur cluster biogenesis machinery, J. Biol. Chem. 298 (2022) 102094.
[203] D.C. Odermatt, K. Gari, The CIA targeting complex is highly regulated and provides two distinct binding sites for client Iron-sulfur proteins, Cell Rep. 18 (2017) 1434–1443.
[204] N. van Wietmarschen, A. Moradian, G.B. Morin, P.M. Lansdorp, E.J. Uringa, The mammalian proteins MMS19, MIP18, and ANT2 are involved in cytoplasmic iron-sulfur cluster protein assembly, J. Biol. Chem. 287 (2012) 43351–43358.
[205] G. Karamanlidis, C.F. Lee, L. Garcia-Menendez, S.C. Kolwicz Jr., W. Suthammarak, G. Gong, M.M. Sedensky, P.G. Morgan, W. Wang, R. Tian, Mitochondrial complex I deficiency increases protein acetylation and accelerates heart failure, Cell Metab. 18 (2013) 239–250.
[206] V. Maione, D. Grifagni, F. Torricella, F. Cantini, L. Banci, CIAO3 protein forms a stable ternary complex with two key players of the human cytosolic iron-sulfur cluster assembly machinery, J. Biol. Inorg. Chem. 25 (2020) 501–508.
[207] E. Urzica, A.J. Pierik, U. Muhlenhoff, R. Lill, Crucial role of conserved cysteine residues in the assembly of two iron-sulfur clusters on the CIA protein Nar1, Biochemistry 48 (2009) 4946–4958.
[208] B. OuYang, L. Wang, S. Wan, Y. Luo, L. Wang, J. Lin, B. Xia, Solution structure of monomeric human FAM96A, J. Biomol. NMR 56 (2013) 387–392.
[209] K.E. Chen, A.A. Richards, J.K. Ariffin, I.L. Ross, M.J. Sweet, S. Kellie, B. Kobe, J. L. Martin, The mammalian DUF59 protein Fam96a forms two distinct types of domain-swapped dimer, Acta Cryst. D 68 (2012) 637–648.
[210] V. Maione, F. Cantini, M. Severi, L. Banci, Investigating the role of the human CIA2A-CIAO1 complex in the maturation of aconitase, Biochim. Biophys. Acta 2018 (1862) 1980–1987.
[211] N.R. Prusty, A. Camponeschi, S. Ciofi-Baffoni, L. Banci, The human YAE1-ORAOV1 complex of the cytosolic iron-sulfur protein assembly machinery binds a [4Fe-4S] cluster, Inorg. Chim. Acta 518 (2021) 1–10.
[212] V.D. Paul, U. Muhlenhoff, M. Stumpfig, J. Seebacher, K.G. Kugler, C. Renicke, C. Taxis, A.C. Gavin, A.J. Pierik, R. Lill, The deca-GX3 proteins Yae1-Lto1 function as adaptors recruiting the ABC protein Rli1 for iron-sulfur cluster insertion, Elife 4 (2015) e08231.
[213] C. Zhai, Y. Li, C. Mascarenhas, Q. Lin, K. Li, I. Vyrides, C.M. Grant, B. Panaretou, The function of ORAOV1/LTO1, a gene that is overexpressed frequently in cancer: essential roles in the function and biogenesis of the ribosome, Oncogene 33 (2014) 484–494.
[214] L. Banci, I. Bertini, S. Ciofi-Baffoni, T. Kozyreva, K. Zovo, P. Palumaa, Affinity gradients drive copper to cellular destinations, Nature 465 (2010) 645–648.
[215] D.L. Huffman, T.V. O'Halloran, Energetics of copper trafficking between the Atx1 Metallochaperone and the intracellular copper-transporter, Ccc2, J. Biol. Chem. 275 (2000) 18611–18614.